The HPA stress axis shapes aging rates in long-lived, social mole-rats

Arne Sahm[1#], Steve Hoffmann[1], Philipp Koch[2], Yoshiyuki Henning[3], Martin Bens[4], Marco Groth[4], Hynek Burda[5,6], Sabine Begall[5], Saskia Ting[7], Moritz Goetz[7], Paul Van Daele[8], Magdalena Staniszewska[9], Jasmin Klose[9], Pedro Fragoso Costa[9], Matthias Platzer[1], Karol Szafranski[2,*], Philip Dammann[5,10,*]

[1] Computational Biology Group, Leibniz Institute on Aging – Fritz Lipmann Institute, Jena, Germany.

[2] Core Facility Life Science Computing, Leibniz Institute on Aging – Fritz Lipmann Institute, Jena, Germany.

[3] Institute of Physiology, University Hospital, University of Duisburg-Essen, Essen, Germany.

[4] Core Facility Sequencing, Leibniz Institute on Aging – Fritz Lipmann Institute, Jena, Germany.

[5] Department of General Zoology, Faculty of Biology, University of Duisburg-Essen, Essen, Germany.

[6] Department of Game Management and Wildlife Biology, Faculty of Forestry and Wood Sciences, Czech University of Life Sciences, Prague, Czech Republic.

[7] Institute of Pathology and Neuropathology, University Hospital, University of Duisburg-Essen, Essen, Germany.

[8] University of South Bohemia, Department of zoology Branišovská 1760, 370 05 České Budějovice, Czech Republic

[9] Department of Nuclear Medicine, University Hospital, University of Duisburg-Essen, Essen, Germany.

[10] Central Animal Laboratory, University Hospital, University of Duisburg-Essen, Essen, Germany.

[#] Corresponding author (email: arne.sahm@leibniz-fli.de)

*shared senior authorship

Abstract

Sexual activity and/or reproduction doubles life expectancy in the long-lived rodent genus *Fukomys*. To investigate the molecular mechanisms underlying this phenomenon, we analyzed a total of 636 RNA-seq samples across 15 tissues. This analysis suggests that the differences in life expectancy between reproductive and non-reproductive mole-rats are mainly caused by critical changes in the regulation of the hypothalamic-pituitary-adrenal stress axis, which we further substantiate with a series of independent evidence. In accordance with previous studies, the up-regulation of the proteasome and

several so-called "anti-aging molecules", such as DHEA, is also linked with enhanced life expectancy. On the other hand, several our results oppose crucial findings in short-lived model organisms. For example, we found the up-regulation of the IGF1/GH axis and several other anabolic processes to be compatible with a considerable lifespan prolongation. These contradictions question the extent to which findings from short-lived species can be transferred to longer-lived ones.

Keywords

lifespan, *Fukomys*, hypothalamic–pituitary–adrenal axis, ACTHR, ACTH, DHEA, IGF1, growth hormone, differential gene expression

Introduction

Most of our current understanding of the underlying mechanisms of aging comes from short-lived model species. It is, however, still largely unclear to what extent insights obtained from short-lived organisms can be transferred to long-lived species, such as humans (Parker et al. 2004; Keller and Jemielity 2006). Comparative approaches, involving species with particularly long healthy lives and seeking the causative mechanisms that distinguish them from shorter-lived relatives try to overcome this limitation (Austad 2009). Many studies that involved organisms with particularly long lifespans, e.g., queens in social hymenoptera, birds, bats, African mole-rats, and primates, have produced findings that were not always congruent with established aging theories (Keller and Jemielity 2006; Austad 2009; Salmon et al. 2009; Austad 2011; Dammann 2017; Bens et al. 2018).

Species comparisons, however, also have their limitations. Many observed differences between species with differing lifespans are influenced by phylogenetic constraints, eco-physiological differences, or both, rather than being causal for the species-specific differences in aging rate and longevity. Therefore,

47 the results mentioned above would gain much more value if they could be confirmed or falsified in a
48 system in which it is unnecessary to cross the species border, that is, in a species that contains easily
49 distinguishable cohorts with high vs. low longevity.

50 Bimodal aging occurs naturally in the genus *Fukomys* from the rodent family Bathyergidae (African mole-
51 rats). These animals live in families (often called colonies) of usually consisting of 9 to 16 individuals
52 (Sichilima et al. 2008; Skliba et al. 2012), although single families may occasionally grow considerably
53 larger in some species (Jarvis and Bennett 1993; Scharff et al. 2001). Regardless of group size, an
54 established family typically consists of only one breeding pair (the founders of the family, often called
55 king/queen) and their progeny from multiple litters (often called workers). Because of strict avoidance
56 of incest (Burda 1995), the progeny do not engage in sexual activity in the confines of their natal family,
57 even after reaching sexual maturity. Hence, grown *Fukomys* families are characterized by a subdivision
58 into breeders (the founder pair) and non-breeders (all other family members). Interestingly, breeders
59 reach the age of 20 years or more in captivity, whereas non-breeders usually die before their tenth birth
60 date (Fig. 1A). This divergence of survival probabilities between breeders and non-breeders is found in
61 all *Fukomys* species studied so far, irrespective of sex. Because no difference in diet or workload has
62 been observed between breeders and non-breeders in captivity, status-specific changes of gene
63 expression after the transition from non-breeder to breeder are considered the most likely explanation
64 of the differing lifespans (Dammann and Burda 2006; Dammann et al. 2011).

65 In the wild, non-breeders must meet a member of another family by chance to ascend to breeder status;
66 in captivity, the establishment of new breeder pairs is subject to human control. Allowing an animal to
67 breed in captivity can be regarded as a simple experimental intervention that results in an extension of
68 life expectancy of approximately 100%. This extension is far more than most experimental interventions
69 in vertebrates can achieve e.g. by caloric restriction (e.g., (Carmona and Michan 2016)) or diets

70 containing resveratrol or rapamycin (e.g., (Valenzano et al. 2006; Johnson et al. 2013)). Furthermore,
71 this relative lifespan extension starts from a non-breeder lifespan that is already more than twice as long
72 as that of the mammalian model organisms most widely used in aging research, such as mice or rats.

73 Until now, relatively few studies have addressed the potential mechanisms behind this natural status-
74 dependency of aging in *Fukomys* sp. Contrary to the predictions of both the advanced glycation
75 formation theory (Morimoto and Cuervo 2009) and the oxidative stress theory of aging (Harman 1956;
76 Harman 2001), markers of protein cross-linking and -oxidation were surprisingly higher in breeders of
77 Ansell´s mole-rats (*F. anselli*) than in age-matched non-breeders (Dammann et al. 2012). On the other
78 hand, in the Damaraland mole-rat (*F. damarensis*), oxidative damage to proteins and lipids was
79 significantly lower in breeding females than in their non-reproductive counterparts (Schmidt et al.
80 2014), a finding that is compatible with the oxidative stress theory of aging. In good agreement with
81 their overall longevity irrespective of social status, Ansell´s mole-rats produce less thyroxine (T4) and
82 recruit smaller proportions of their total T4 resources into the active unbound form than do euthyroid
83 mammals. Still, nonetheless the levels of unbound T4 (fT4) do not explain the intraspecific differences in
84 aging rates between *F. anselli* breeders and non-breeders, because the levels of this hormone did not
85 differ between the two cohorts (Henning et al. 2014). Closely connected to the topic of this paper is the
86 finding, that non-breeding giant mole-rats (*F. mechowii*) maintain fairly stable gene expression into
87 relative old ages, quite in contrast to the shorter-lived Norway rat (Sahm et al. 2018a). It is, however,
88 still unclear what happens on the gene expression level when an individual attains breeding status.

89 Interestingly, a recent study by (Bens et al. 2018) found that the longest-lived rodent, the naked mole-
90 rat *Heterocephalus glaber*, tended globally to show opposite changes in the transition from non-
91 breeders to breeders compared to shorter-lived guinea pigs. *Heterocephalus* and *Fukomys* are similar in
92 their mating and social behavior, but differences appear to exist regarding the effect of breeding on

93 aging rates: until very recently, naked mole-rat non-breeders have been reported to be as long-lived as
94 breeders (Sherman and Jarvis 2002; Buffenstein 2008). In 2018, a lifespan advantage of breeders over
95 non-breeders was reported in females (but not males), yet the divergence of the two groups appeared
96 to be considerably smaller than in *Fukomys* (Ruby et al. 2018) and underlying data is being debated
97 (Dammann et al. 2019). In summary, status-dependent aging is either absent in *Heterocephalus* or less
98 pronounced than in *Fukomys*.

99 In this paper, we make use of the bimodal aging pattern in two *Fukomys* species (*F. mechowii* and *F.*
100 *micklemi*, Fig. 1A) by comparing the gene expression profiles of breeders (n=24) and age-matched non-
101 breeders (n=22) in 16 organs or their substructures (hereinafter referred to as tissues, Fig. S1, Fig. 1B).
102 Our main aim was to identify genes and pathways whose transcript levels are linked to the status-
103 dependent aging-rates and to relate these patterns to insights into aging research obtained in shorter-
104 lived species.

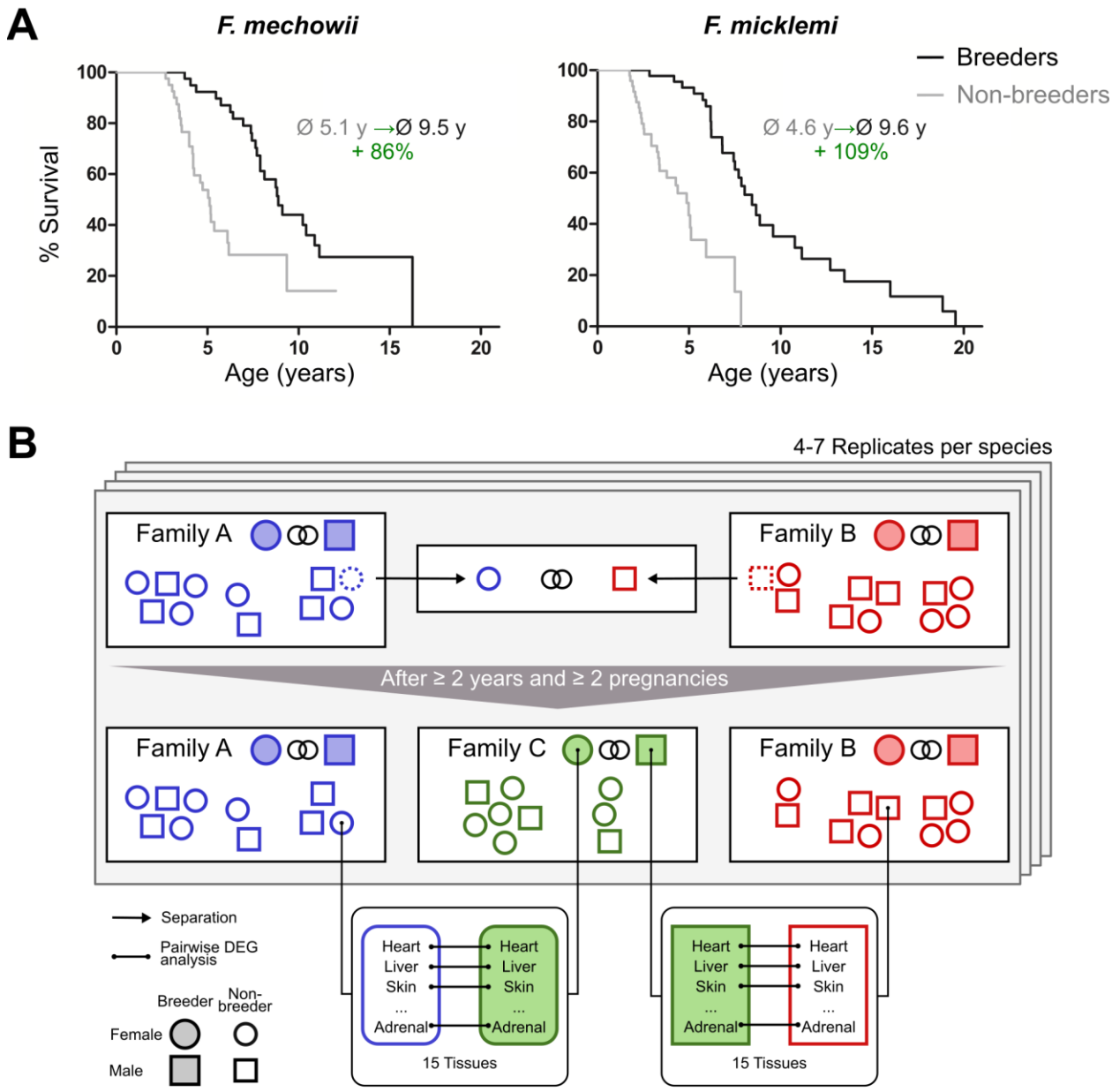

Figure 1. Motivation (A) and principle of the experimental setup (B). **A)** For both species of the *Fukomys* genus that were examined in this study – *F. mechowii* and *F. micklem*i – it was shown that, in captivity, breeder live significantly longer than non-breeders. Lifespan data were redrawn from Dammann & Burda and Dammann et al. (Dammann and Burda 2006; Dammann et al. 2011). **B)** Schematic overview of animal treatments. Non-breeders (open shapes) are offspring of the breeder pair of their family (filled shapes) and do not mate with other members of the same family because of incest avoidance in *Fukomys* (Burda 1995). Therefore, non-breeders of opposite

112 sexes were taken from different families – labeled as “Family A” (blue) and “Family B” (red) – and permanently
113 housed in a separate terrarium. The two unrelated animals mated with each other, thus producing offspring and
114 becoming breeders of the new “Family C” (green). In addition to the animals that were promoted to be slower-
115 aging breeders, age-matched controls that remained in the faster-aging non-breeders of “Family A” and “Family B”
116 were included in our study – in most cases full siblings (ideally litter mates) of the respective new breeders. After
117 at least two years and two pregnancies in “Family C”, breeders from “Family C” and their controls from Colonies A
118 and B were put to death, and tissues were sampled for later analysis, that included identification of differentially
119 expressed genes (DEGs). The shown experimental scheme was conducted with 5 to 7 (median 6) specimens per
120 cohort (defined by breeding status, sex, species) and 12 to 15 tissues (median 14) per specimen: in total, 46
121 animals and 636 samples.

122 Results

123 We measured gene expression differences between breeders and non-breeders in two African mole-rat
124 species, *F. mechowii* and *F. micklemi*. Altogether, we performed RNA-seq for 636 tissue samples
125 covering 16 tissue types from both species, sexes, and reproductive states (breeders and non-breeders).
126 Each of the four groups (male/female breeders/non-breeders) of each species consisted of 5 to 7
127 animals (see Tables S1 –S5 for sample sizes, animal data, and pairing schemes). For each tissue, we
128 conducted a multi-factorial analysis of differentially expressed genes (DEGs): the analysis was based on
129 the variables reproductive state, sex, and species. During this exercise, we focused on the differences
130 between slower-aging breeders and faster-aging non-breeders. This approach increases our statistical
131 power by giving us a four-fold increase of sample size in comparison to species- and sex-specific breeder
132 vs. non-breeder analyses. At the same time, we can additionally reduce the number of false-positive
133 DEGs by restricting the analysis to those breeding status-related genes that show the same direction in

134 both sexes and both species. We deliberately focused on those genes to concentrate our study on
135 universal mechanisms that hold for both sexes and species.

136 To globally quantify the transcriptomic differences between the reproductive states, we performed
137 three analyses: clustering of the samples based on pairwise correlation, principal variant component
138 analysis, and an overview of the number of DEGs between reproductive states in comparison to DEGs
139 between species and sex. Clustering of the samples based on pairwise correlations showed a full
140 separation of the two species at the highest cluster level (Fig. S1). Below that level, an almost complete
141 separation according to tissues was observed. Within the tissue clusters, the samples did not show a
142 clear-cut separation between sex or breeder/non-breeder status. Accordingly, a principal variance
143 component analysis showed that species, tissue, and the combination of both variables accounted for
144 98.4 % of the total variance in the data set; individual differences explained 1.4 % of the variance, and
145 only 0.004 % was explained by breeder/non-breeder status (Fig. 2A). Regarding the numbers of DEGs,
146 we found – unsurprisingly considering the aforementioned facts –by far the highest number of DEGs in
147 the species comparison (Fig. 2B). Although in almost every examined tissue the numbers of detected
148 DEGs were also high between sexes, most tissues exhibited very few DEGs due to breeder/non-breeder
149 status. Exceptions were liver, spleen, ovary and, especially, tissues of the endocrine system (adrenal
150 gland, pituitary gland, thyroid), in which the number of DEGs between breeders and non-breeders
151 ranged from more than sixty to several thousand.

Figure 2. Total variance distribution (A) and numbers of differentially expressed genes (B). **A)** Relative contribution of the model factors (breeding status, sex, species, tissue) and their combinations (:) to the total variance in the examined data set. The relative contributions were determined by principal variance component analysis. **B)** Numbers of identified differentially expressed genes per tissue and model factor (first column, species; second, sex; third, status). Stacked bars indicate the proportions of up- and down-regulated genes (red and green, respectively; directions: *F. mechowii* vs. *F. micklemi*, female vs. male, breeder vs. non-breeder).

Next, we evaluated the relevance of reproductive status DEGs for aging and aging-related diseases. For this analysis, we first determined overlaps by using the Digital Aging Atlas (DAA) – a database of genes that show aging-related changes in humans (Craig et al. 2015). Across species and sexes, significant

162 overlaps (FDR < 0.05, Fisher's exact test) with the DAA were found in three tissues: adrenal gland, ovary
163 and pituitary gland (false discovery rate [FDR] = 0.005, each; Fig. 3A). Among these three endocrine
164 tissues, the DEGs of the ovaries overlapped significantly with those from adrenal ($p=2.8*10^{-27}$) and
165 pituitary glands (p=0.005), but there was no significant overlap between the two glands (Fig. 3A). Thus,
166 together, we found indications for aging-relevant expression changes after the transition from non-
167 breeders to breeders in three tissues of the endocrine system, which presumably affect separate
168 aspects of aging in adrenal and pituitary glands.

169 Moreover, we compared the DEGs with respect to the reproductive status that we identified in *Fukomys*
170 with regard to their direction to transcript-level changes observed in similar experiments using naked
171 mole-rats and guinea pigs (Bens et al. 2018). The direction of the status-dependent DEGs regulation in
172 *Fukomys*, as found in this study, was significantly more often the same rather than opposite as in the
173 naked mole-rat (females, 60 %, $p=5.2*10^{-58}$; males, 62 %, $p=10^{-44}$ for females, Fig.3B, Table S6). In the
174 guinea pig, on the contrary, the *Fukomys* reproductive status DEGs were significantly more often
175 regulated in the opposite direction (females, 57 %, $p=9*10^{-25}$; males, 59 %, $p=4.7*10^{-23}$, Fig. 3B, Table
176 S6). Thus, at the single-gene level, the expression changes linked to reproductive status may affect
177 lifespan differently in long-lived African mole-rats than in shorter-lived guinea pigs.

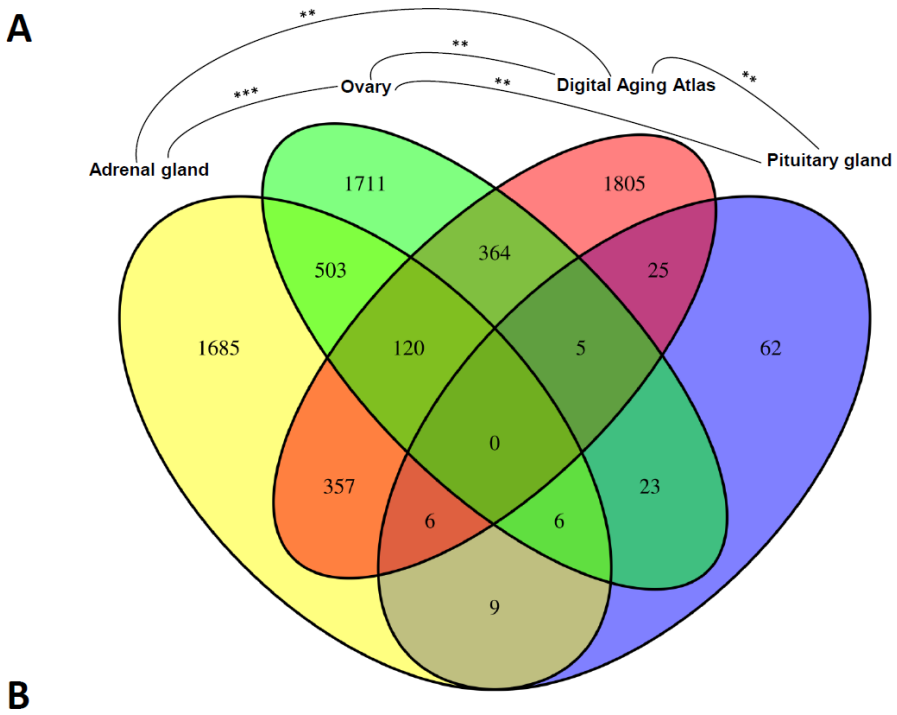

	NMR ♀	NMR ♂	GP ♀	GP ♂
Same	3561	2060	2521	1352
Opposite	2332	1225	3305	1917
P-value	$5.2*10^{-58}$	$1*10^{-44}$	$9*10^{-25}$	$4.7*10^{-23}$

Figure 3. Assessment of the aging relevance of genes that are differentially expressed between breeders and non-breeders. **A)** For each tissue, we separately tested whether the identified differentially expressed genes between status groups significantly overlapped with the genes within the Digital Aging Atlas database (Fisher's exact test, FDR < 0.05). Significant overlaps were found for three tissues: adrenal gland, ovary and pituitary gland. The Venn-diagram depicts the overlaps of these three tissues with the Digital Aging Atlas and with each other (** : FDR < 0.01; *** : FDR < 0.001). **B)** A similar experiment comparing the transcriptomes of breeders versus non-breeders was recently conducted in naked mole-rats (NMRs) and guinea pig (GPs) (Bens et al. 2018). For NMR there is also evidence that breeders have a (slightly) longer lifespan than non-breeders, whereas for GP the opposite is assumed (Bens et al. 2018; Ruby et al. 2018). Across ten tissues that were examined in both studies, the analysis determined whether status-dependent differentially expressed genes identified in the current study were regulated in the same or opposite direction in NMR and GP (Table S6). The listed p-values (two-sided binomial exact test; hypothesized probability, 0.5) describe how extremely the ratio of genes expressed in the same and opposite directions deviates from a 50:50 ratio. Green and orange indicate the majority and minority of genes within a comparison, respectively. Figure created with BioRender.com.

192 Beyond the single-gene level, we aimed to identify metabolic pathways and biological functions whose
193 gene expression significantly depends on reproductive status. For this, we used Kyoto Encyclopedia of
194 Genes and Genomes (KEGG) pathways (Kanehisa et al. 2017), and Molecular Signatures Database
195 (MSigDB) hallmarks (Liberzon et al. 2015) as concise knowledge bases. We used a known method that
196 combines all p-values of genes in a given pathway in a threshold-free manner. The advantage of this
197 approach is that it bundles the p-values from test results of individual gene expression differences at the
198 level of pathways (see Methods section for details). Altogether, the gene expression of 55 KEGG
199 pathways and 41 MSigDB hallmarks was significantly affected by reproductive status in at least one
200 tissue (Fig. S3 and S4). Because the individual interpretation of each of these pathways/hallmarks would
201 go beyond the scope of this study, we focus here on those 14 pathways and 13 hallmarks that were
202 significantly different between breeders and non-breeders (FDR < 0.1) in a global analysis across all
203 tissues (Fig. 4). Because many pathways are driven mainly by gene expression in subsets of tissues, we
204 weighted gene-wise the differential expression signals from the various tissues by the respective
205 expression levels in the tissues. For instance, the expression level of the growth hormone (GH) gene *GH1*
206 is known to be almost exclusively expressed in the pituitary glands. In our data set the *GH1* level of the
207 pituitary gland accounted for 99.96 % of the total *GH1* across all tissues. Accordingly, in pathways that
208 contain *GH,* our weighted cross-tissue differential expression signal for this gene is almost exclusively
209 determined by the pituitary gland. On the contrary, a differential expression signal of this gene in
210 another tissue with a very low fraction of the gene's total expression would have almost no impact on
211 the weighted cross-tissue level – even if that signal were very strong (see Methods section for details).

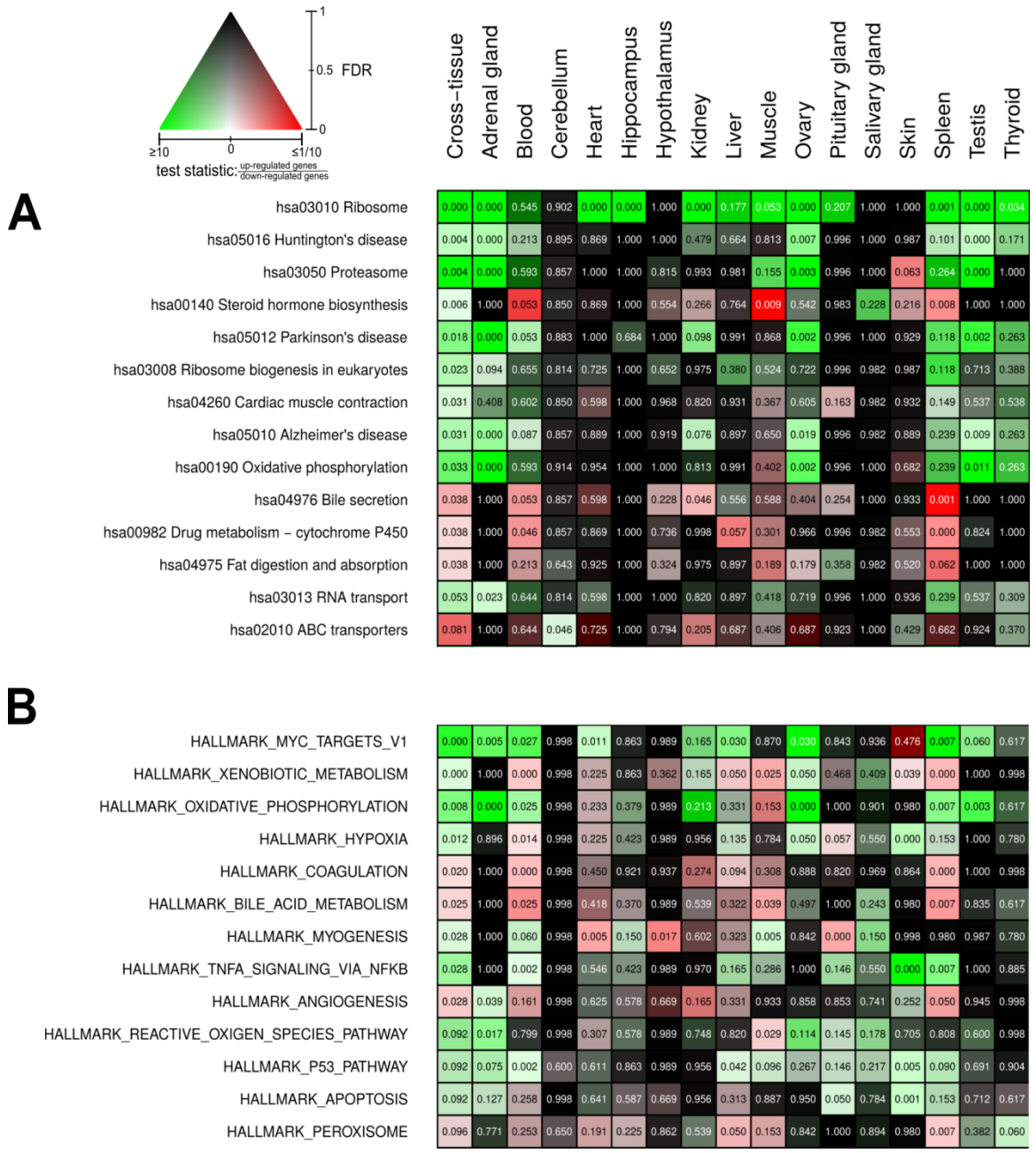

Figure 4. Pathways and metabolic functions enriched for status-dependent differential gene expression. Shown are all Kyoto Encyclopedia of Genes and Genomes (KEGG) pathways (**A**) and Molecular Signatures Database (MSigDB) hallmarks (**B**) that are enriched for differential gene expression between breeders and non-breeders at the weighted cross-tissue level (false discovery rate [FDR], < 0.1). The numbers within the cells give the FDR, i.e., the multiple testing corrected p-value, for the respective pathway/hallmark and tissue. As indicated by the color key, red and green stand for up- or down-regulated in breeders, respectively. White indicates a pathway/hallmark that is significantly affected by differential expression and whose signals for

219 up- and down-regulation are approximately balanced. Dark colors up to black mean that there is little or no evidence that the
220 corresponding pathway/hallmark is affected by differential gene expression. Figures S3 and S4 provide detailed overviews of all
221 pathways/hallmarks that are enriched in at least one tissue for status-dependent differential expression signals.

222 We found strong indications for increase in the activity of certain anabolic functions in breeders:
223 Ribosomal protein expression (hsa03010 Ribosome, hsa03008 Ribosome biogenesis in eukaryotes, Fig.
224 4A) was elevated in most tissues (and accordingly also in the weighted cross-tissue analysis). In MSigDB
225 hallmarks, the strongest enrichment signal came from MYC targets (HALLMARK_MYC_TARGETS_V1),
226 which can largely be considered a reflection of enhanced ribosomal protein expression and the fact that
227 MYC is a basal transcription factor up-regulating genes involved in protein translation ((Hofmann et al.
228 2015), Fig. 4B). In functional correspondence, we observed an increase in the expression of
229 mitochondrial respiratory chain components (hsa00190 Oxidative Phosphorylation,
230 HALLMARK_OXIDATIVE_PHOSPHORYLATION, Fig. 4A,B). We also found strong indications for increased
231 protein degradation (hsa03050 PROTEASOME, Fig. 4A). This weighted cross-tissue signal was, in contrast
232 to the situation regarding ribosomes, driven mainly by two tissue types: the adrenal gland and the
233 gonads.

234 To examine whether the simultaneous up-regulation of the ribosome, proteasome, and oxidative
235 phosphorylation is a coordinated regulation, we performed a weighted gene co-expression network
236 analysis (WGCNA) (Langfelder and Horvath 2008) from our gene count data and examined the
237 connectivity between pairs of those KEGG pathways flagged in the weighted cross-tissue analysis. We
238 found that the expression of ribosomal genes (hsa03010) was significantly linked to those of ribosome
239 biogenesis (hsa03008, FDR=$4.59*10^{-3}$), oxidative phosphorylation (hsa00190, FDR=$4.05*10^{-4}$), and
240 proteasome (hsa03050, FDR=$4.59*10^{-3}$), whereas no other examined pathway pair exhibited a
241 significant connectivity (Fig. S5). Interestingly, ribosome, proteasome, and oxidative phosphorylation

242 pathways also shared other characteristics of their differential expression signals: subtle fold-changes,
243 that is, up-regulation of 3 to 9 % on average. Thus, statistically significant signals at the pathway level
244 resulted from relatively small shifts in all genes of these pathways in a seemingly coordinated manner
245 and across multiple tissues (Data S1). In addition, ribosome (hsa03010, in ovary), proteasome
246 (hsa03050, in ovary and adrenal gland), and RNA-transport (hsa03013, in adrenal gland) are enriched in
247 those *Fukomys* status-dependent DEGs that show, in a similar experimental setting (Bens et al. 2018),
248 the same direction in both naked mole-rat sexes and the opposite direction in both guinea pig sexes
249 (FDR < 0.05, Fisher's exact test).

250 The myogenesis hallmark (Fig. 4B) was also found to be up-regulated in breeders. Expectedly, this
251 weighted cross-tissue result was driven mainly by differential expression signals from muscle tissue:
252 muscle from all tissues exhibited the lowest p-value (Fig. 4A), and 15 of 20 up-regulated genes that
253 contributed most to the weighted cross-tissue differential myogenesis signal exhibited their highest
254 expression in muscle. These genes were involved mainly in calcium transport or part of the fast-skeletal
255 muscle-troponin complex (Data S1). A clear exception of this muscle-dominated expression is found in
256 the gene that exhibited the highest relative contribution to the differential myogenesis signal, *insulin-*
257 *like growth factor 1* (*IGF1*). This gene was found to be expressed most strongly in ovary and liver and
258 was strongly up-regulated in the breeders´ ovaries and adrenal glands (Table 1). *IGF1* codes for a well-
259 known key regulator of anabolic effects such as cell proliferation, myogenesis, and protein synthesis
260 (Schiaffino and Mammucari 2011; Jung and Suh 2014) and has a tight functional relation to GH (gene:
261 *GH1*) another key anabolic regulator upstream of *IGF1*; together, these factors form the so-called
262 GH/IGF1 axis (Cannata et al. 2010; Junnila et al. 2013; Bodart et al. 2015; Raisingani et al. 2017; Carotti
263 et al. 2018; Lozier et al. 2018). Also, *GH1* was strongly up-regulated in breeders in its known principal
264 place of synthesis, the pituitary gland (Table 1).

265 With xenobiotic metabolism and TNF-α-signaling, two defense hallmarks were also found to be up-
266 regulated in breeders by the weighted cross-tissue analysis (HALLMARK_XENOBIOTIC_METABLISM and
267 HALLMARK_TNFA_SIGNALING_VIA_NFKB, Fig. 4B). The up-regulation of the reactive oxygen species
268 (ROS) hallmark comprising genes coding for proteins that detoxify ROS
269 (HALLMARK_REACTIVE_OXYGEN_SPECIES_PATHWAY, Fig. 4B) falls into a similar category.

270 Another interesting aspect that was found to be significantly altered in breeders is steroid hormone
271 biosynthesis (hsa00140 Steroid hormone biosynthesis, Fig. 4A). In this case, both up- and down-
272 regulated genes were in the pathway, and their absolute fold-changes were roughly balanced. Steroid
273 hormones, on the one hand, comprise sex steroids – because these hormones are important players in
274 sexual reproduction, such differences should be expected given the experimental setup. On the other
275 hand, the class of steroid hormones – corticosteroids – has regulatory functions in metabolism, growth,
276 and the cardiovascular system, as well as in the calibration of the immune system and response to stress
277 (Liu et al. 2013). The most influential contributor to the differential pathway signal by far on the
278 weighted cross-tissue level was *CYP11A1,* which codes for the (single) enzyme that converts cholesterol
279 to pregnenolone. This is the first and rate-limiting step in steroid hormone synthesis (Miller and Auchus
280 2011). Because *CYP11A1* was found to be up-regulated in breeders in its main places of synthesis – the
281 gonads and the adrenal gland (Table 1) – it can be assumed that the total output of steroid hormone
282 biosynthesis in breeders is increased. The pattern of up- and down-regulation on the KEGG pathway,
283 however, suggests that sex steroids especially are produced at a higher rate in breeders whereas
284 circulating levels of glucocorticoids – such as cortisol – should be lower than in non-breeders (Fig. S6;
285 see also our discussion on ACTH-R below).

286 Finally, several pathways flagged by the weighted cross-tissue analysis seem to be derivatives of the
287 above-mentioned differentially expressed pathways instead of representing altered functions on their

288 own. For example, Huntington's (hsa05016), Parkinson's (hsa05012), and Alzheimer's (hsa05010)
289 diseases could, in principle, be interpreted as highly relevant for aging and lifespan. A closer inspection
290 of these pathways reveals, however, that the genes of the mitochondrial respiratory chain – which is the
291 core of the oxidative phosphorylation pathway – are in all three cases the main contributors to the
292 respective differential expression signals (Fig. S7-S9, Data S1). Similarly, we see in the case of fat
293 digestion (hsa04975 Fat digestion and absorption) that two of the three largest contributors to the
294 differential expression signal of that pathway – *ABCG8* and *SCARB1* – are directly involved in the
295 transport of cholesterol (Liu et al. 2008; Wang et al. 2015). Therefore, it seems likely that this signal is an
296 expression of the altered steroid hormone biosynthesis rather than indicating altered fat digestion.

297 **Table 1.** Top ten genes regarding weighted cross-tissue differential expression signal.

	Weighted cross-tissue			Tissue with highest expression			
	P-value	FDR	Log2-foldchange*	Tissue	% of cross-tissue Expression	FDR	Log2-foldchange*
SULT2A1	0.00E+00	0.000	-3.19	Liver	97.42	5.27E-06	-3.26
MC2R	6.00E-06	0.046	-0.53	Adrenal gland	89.53	8.78E-05	-0.56
INHA	1.60E-05	0.081	1.57	Ovary	67.91	1.54E-05	2.22
INHA – tissue with 2nd highest expression				Testis	27.61	0.56	0.21
CYP11A1	5.90E-05	0.224	0.61	Ovary	45.55	5.49E-05	0.91
CYP11A1 – tissue with 2nd highest expression				Adrenal gland	43.63	1.48E-03	0.47
NLRP14	1.17E-04	0.355	-0.80	Ovary	68.98	2.84E-05	-1.25
NLRP14– tissue with 2nd highest expression				Testis	18.67	0.54	0.19
GH	2.58E-04	0.618	0.45	Pituitary gland	99.96	1.99E-02	0.45
IGF1	3.62E-04	0.618	0.59	Ovary	51.73	1.20E-04	0.76
IGF1– tissue with 2nd highest expression				Liver	36.28	0.39	0.24
ZP4	3.74E-04	0.618	-1.16	Ovary	95.30	1.99E-03	-1.23
TCL1A	5.33E-04	0.618	-1.05	Ovary	90.12	2.14E-03	-1.18
PNLIPRP2	5.69E-04	0.618	1.36	Ovary	76.08	2.23E-03	1.65

298 * Direction: breeder/non-breeder
299 Note – tissues are listed if they contribute at least 10% to cross-tissue expression

300 Interestingly, three genes, which we had already mentioned as potential regulators during the pathway
301 analysis, also appeared among the ten most clearly altered genes on the weighted cross-tissue level:

302 *GH1, IGF1,* and *CYP11A1* (Table 1). The top two among these ten are *sulfotransferase family 2A member*
303 *1* (*SULT2A1*) and *melanocortin 2 receptor* (*MC2R*). SULT2A1 is the main catalyzer of the sulfonation of
304 the steroid hormone dehydroepiandrosterone (DHEA) to its non-active form DHEA-S (Hammer et al.
305 2005). DHEA has repeatedly been proposed to be an "anti-aging hormone" because its levels are
306 negatively associated with chronological aging (Baulieu 1996; Celec and Starka 2003; Rutkowski et al.
307 2014). We found that *SULT2A1* is strongly down-regulated in breeders', liver which is also the main
308 location of its enzymatic action. The second candidate, *MC2R*, encodes the adrenocorticotropin (ACTH)-
309 receptor, which is the main inducer of glucocorticoid synthesis and a crucial component of the
310 hypothalamic–pituitary–adrenal (HPA) axis (Walker et al. 2015). In humans and many other mammals,
311 prolonged glucocorticoid excess leads to Cushing's syndrome. Affected individuals exhibit muscle
312 weakness, immune suppression, impairment of the GH/IGF1 axis, higher risk of diabetes, cardiovascular
313 disease (hypertension), osteoporosis, decreased fertility, depression, and weight gain (Chabre 2014;
314 Ferrau and Korbonits 2015). The large overlap of these symptoms with those of aging could explain to
315 some extent that Cushing's syndrome patients exhibit considerably higher mortality rates (Etxabe and
316 Vazquez 1994). We hypothesized that the increased expression of the ACTH receptor in *Fukomys* non-
317 breeders can cause similar expression patterns and consequences (Fig. 5).

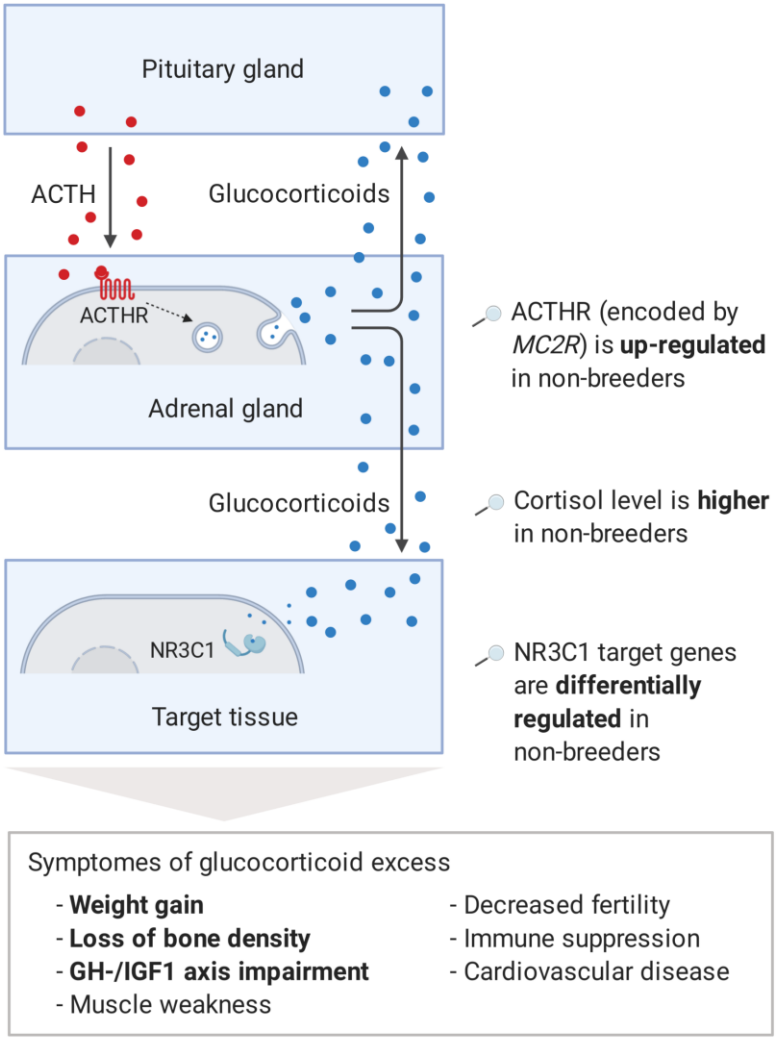

318

319 **Figure 5.** Model of the stress axis as a key mechanism for status-dependent lifespan differences in *Fukomys*. From a wide range
320 of mammals, including humans (Ferrau and Korbonits 2015), dogs (Kooistra and Galac 2012), horses (McCue 2002), cats (Meijer
321 et al. 1978), and guinea pigs (Zeugswetter et al. 2007), it is known that chronic glucocorticoid excess leads to a number of
322 pathologic symptoms that largely overlap with those of aging and result in considerably higher mortality rates for affected
323 individuals (Etxabe and Vazquez 1994#808). The most common cause of chronic glucocorticoid excess is excessive secretion of
324 the adrenocorticotropic hormone (ACTH) by the pituitary gland. ACTH is transported via the blood to the adrenal cortex where
325 it binds to the ACTH-receptor (ACTHR; encoded by the gene *MC2R*) which induces the production of glucocorticoids, especially
326 cortisol. Glucocorticoids are transported to the various tissues, where they exert their effect by activating the glucocorticoid
327 receptor (NR3C1) that acts as a transcription factor and regulates hundreds of genes. The constant overuse of this

328 transcriptional pattern eventually leads to the listed symptoms. Our hypothesis is that the permanent, high expression of the
329 ACTH-receptor in *Fukomys* non-breeders causes effects similar to those known from overproduction of the hormone. In line
330 with this hypothesis, i) cortisol levels are increased in non-breeders and ii) target genes of the glucocorticoid-receptor are
331 highly enriched for status-dependent differential gene expression. Furthermore, the animals were examined for common
332 symptoms of chronic glucocorticoid excess: iii) non-breeders gained more weight during the experiment than breeders, iv)
333 exhibited lower bone density at the end of the experiment, and v) lower gene expression in the GH-/IGF1 axis than breeders.

334 We tested this hypothesis (Fig. 5) by checking five of its key predictions. Altered *MC2R* expression (Fig.
335 6A) coincides with higher cortisol levels in hair samples from non-breeding *F. mechowii* than in those
336 from breeders of the same species (Begall et al., in prep.). Furthermore, glucocorticoids such as cortisol
337 exert their effect by binding to the glucocorticoid receptor that, in turn, acts as a transcription factor for
338 many genes (Gjerstad et al. 2018). We tested whether the expression of targets of the glucocorticoid-
339 receptor (NR3C1) was significantly altered throughout our data using two gene lists (Phuc Le et al. 2005):
340 about three hundred direct target genes of the receptor that were identified by
341 chromatinimmunoprecipitation (i), and about 1300 genes that were found to be differentially expressed
342 depending on the presence or absence of exogenous glucocorticoid (ii). Both gene lists were found to be
343 significantly affected by differential expression at the weighted cross-tissue level (I, $p=0.001$; ii, $p<10^{-9}$)
344 as well as in 5 (i) and 8 (ii) single tissues (Table S7, S8). In line with our hypothesis, we observed that the
345 weight gain in non-breeders was, on average, twice as strong compared to the weight gain in breeders
346 during the experiment ($p=7.49*10^{-3}$,type II ANOVA, Fig. 6B). In addition, we found a subtle but
347 significant influence of reproductive status on the density of the vertebrae': the vertebrae of breeders
348 were slightly denser than those of age-matched non-breeders ($p=0.03$ for vertebra T12 only, and $p=0.01$
349 across all examined vertebrae L1, L2, and T12; ANOVA, Fig. 6C, Table S11).

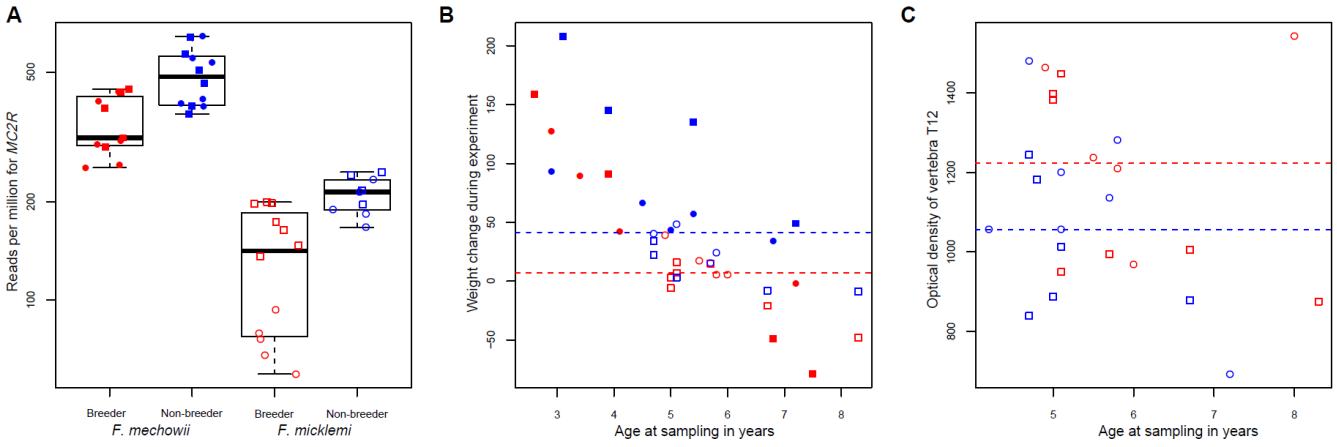

Figure 6. *MC2R* gene expression and physiological measurements. **A)** Gene expression of *MC2R*, coding for the ACTH receptor, in breeders and non-breeders of *Fukomys mechowii* and *Fukomys micklemi*. **B)** Weight gain of the animals during the experiment. **C)** Measured optical densities of vertebra T12 of *Fukomys micklemi* breeders and non-breeders. Red, breeders; blue, non-breeders; filled, *F. mechowii*; unfilled, *F. micklemi*; circles, females; squares, males; dashed line, median. Statistically significant differences between breeders and non-breeders were determined with A) DESeq2 (Love et al. 2014) and B+C) analysis of variance with status, species, sex, and age as independent variables (see methods).

Discussion

The vast lifespan differences between *Fukomys* breeders and non-breeders are, according to our RNA-seq data, associated with only subtle global pattern shifts in transcript levels. Concerning the tested explanatory variables (*Fukomys* species, sex, breeding status), we found by far the highest number of DEGs at the level of the species comparison. Although the number of DEGs between the sexes was comparably high in almost each examined tissue, only very few DEGs were found comparing breeders and non-breeders. One exception is the ovary, whose high number of DEGs corresponds well with the disparity in reproductive activity. Other exceptions are liver, spleen, and, especially, the tissues of the endocrine system (adrenal gland, pituitary gland, thyroid), in which the number of DEGs between breeders and non-breeders ranged from more than 100 to more than 2,500.

367 Changes in the gene expression of the endocrine system are well known to play an important role both
368 in sexual maturation an in aging and the development of aging-associated diseases, e.g., diabetes and
369 cardiovascular diseases (Tatar et al. 2003; Chahal and Drake 2007; Jones and Boelaert 2015). This finding
370 fits well with the observation of substantial changes in the endocrine system after the transition from
371 non-breeders to breeders in the related naked mole-rat – one of the key results of a recent study in that
372 species (Bens et al. 2018). The dominance of differential expression in endocrine tissue is also plausible
373 insofar as these tissues exert a strong control function for other tissues via hormone release.

374 Steroid hormone biosynthesis exhibits a bipartite pattern in breeders, with up-regulated sex steroid
375 genes and a simultaneous down-regulation of corticosteroid synthesis genes. The former could be
376 expected as a consequence of sexual activity in breeders. For aging, it is, however, interesting that
377 *SULT2A1*, a gene that codes for the specialized sulfotransferase converting the sex steroid DHEA to its
378 non-active form DHEA-S was found to be heavily down-regulated in breeders. DHEA is the most
379 abundant steroid hormone; it serves as a precursor for sex steroid biosynthesis but also has various
380 metabolic functions on its own (Allolio and Arlt 2002; Webb et al. 2006). DHEA levels decrease
381 continuously during the human aging process to an extent that favors it as an aging biomarker (Maggio
382 et al. 2007; Traish et al. 2011). As a result, an aggressive advertising of DHEA as "anti-aging hormone" in
383 the form of dietary supplements could be observed in recent years (Baulieu 1996; Celec and Starka
384 2003; Webb et al. 2006; Rutkowski et al. 2014). Despite conflicting experimental data from various
385 animal studies and clinical trials, a positive effect of DHEA on human health is frequently considered to
386 be likely in the literature. Large-scale and long-term studies, however, are still pending (Traish et al.
387 2011; Rutkowski et al. 2014; Samaras et al. 2015). Interestingly, DHEA is not only described as an aging
388 marker but also as a marker for clinically relevant glucocorticoid excess (Burkhardt et al. 2013).

389 Regarding corticosteroid synthesis, we hypothesize that the regulation of adrenal gland *MC2R*, coding
390 for the ACTH receptor, is likely to cause a considerable proportion of the overall observed expression
391 patterns and of the lifespan extension in breeders (Fig. 5). As a critical component of the HPA axis, ACTH
392 is a stress hormone that is produced by the pituitary gland and transported by the the blood to the
393 adrenal cortex, where it binds to the ACTH receptor (Fridmanis et al. 2017). Subsequently, the ACTH
394 receptor induces the synthesis of glucocorticoids (Walker et al. 2015), e.g., cortisol, which in turn cause
395 immunosuppressive and various metabolic effects throughout the organism (Becker 2013). Although in
396 many mammals (such as humans, dogs, and guinea pigs) glucocorticoid excess disorder, Cushing's
397 syndrome, is caused by overproduction of the hormone ACTH. Our results for *Fukomys* suggest, that the
398 increased levels of the ACTH receptor may lead to symptoms and expression patterns that could
399 resemble some of molecular and phenotypic aspects of this pathological condition (Fig. 5). Our
400 hypothesis is supported by a number of confirmed downstream effects: the target genes of the
401 glucocorticoid receptor are highly significantly affected by differential gene expression; non-breeder
402 symptoms were similar to those of humans with abnormally elevated glucocorticoid levels: weight gain,
403 decreases in bone density, and impairment of the GH/IGF1 axis (Fig. 5, Fig.6). Interestingly, blocking of
404 the ACTH receptor has been suggested as a treatment for human Cushing's syndrome (Newfield 2010).

405 We looked for evidence of a regulation upstream of the ACTH receptor. Given the known positive
406 feedback loop between the ACTH receptor and its own ligand, decreased ACTH synthesis in breeders
407 would have been an obvious explanation (Imai et al. 2001). We found that the expression of the ACTH
408 polypeptide precursor gene (*POMC*) is unchanged. However, also other post-transcriptional or post-
409 translational mechanisms such as cleaving may influence the ACTH levels in breeders and non-breeders.
410 Of those genes known to be involved in the regulation of *MC2R* (Beuschlein et al. 2001; Lin et al. 2007),
411 we found that only *PRKAR1B* was differentially regulated in the adrenal gland. However, this gene codes

412 for only one of 7 subunits of the involved protein kinase A. Alternative explanations could be that
413 epigenetic modifications, other still unidentified regulators of the transcript level, or both, are
414 responsible for the differential expression.

415 In the circulatory system, represented by blood and spleen, down-regulation of coagulation factors was
416 observed in breeders. Because coagulation factors are known to be up-regulated during aging in humans
417 mice, rats, and even fish, this can be interpreted as a sign of a more juvenile breeders' transcriptome
418 (Ochi et al. 2016; Benayoun et al. 2019). Furthermore, the activity of coagulation factors is associated
419 with a higher risk of coronary heart disease (Lowe and Rumley 2014). However, we found no obvious
420 histopathological lesions in the hearts or other organs (spleen, kidney, liver, lung) of non-breeders..
421 Therefore, if down-regulation of coagulation attentuates the aging process in *Fukomys*, it seems to exert
422 its effect only, if at all, at a latter age not investigated here.

423 Two defense mechanisms were also found to be up-regulated in breeders: xenobiotic metabolism and
424 TNF-α-signaling. Increased TNF-α-signaling often leads to the induction of apoptosis (Annibaldi and
425 Meier 2018). In line with this, we found that apoptosis and P53-signaling were also up-regulated in
426 breeders. Apoptosis is considered an important anti-cancer mechanism (Baig et al. 2016; Pistritto et al.
427 2016). We hypothesize this to compensate cancerogenic effects of the anabolic alterations described
428 above (especially the up-regulation of the GH/IGF1 axis). In line with this, our more than 30 years'
429 breeding history with several *Fukomys* species in Germany and the Czech Republic suggests that
430 breeders are as "cancer-proof" as non-breeders despite their much longer lifespan (own unpublished
431 data and R. Šumbera, personal communication).

432 Many anabolic pathways are up-regulated in breeders across tissues: protein biosynthesis, myogenesis,
433 and the GH/IGF1 axis. In line with this finding and with the fact that protein synthesis consumes 30 to
434 40% of a cell's ATP budget (Hands et al. 2009), we observed increased expression of mitochondrial

435 respiratory chain components, implying an increase in the capacity for cellular ATP production. On the
436 other hand, protein degradation and clearance by the proteasome are also up-regulated in breeders.
437 The fact that the expression of proteasomal genes is significantly linked to the genes of ribosome
438 biogenesis and oxidative phosphorylation indicates that those processes influence, or even trigger, each
439 other and hence are regulated in a coordinated manner in *Fukomys* mole-rats.

440 The results of differential expression of anabolic components such as the GH/IGF1 axis are surprising.
441 They fall within a debate in aging research that has been highly controversial over time: based on the
442 well-known fact that the expression and secretion of GH and IGF1 decline with age in humans and other
443 mammals (Bartke 2019), Rudman *et al*. administered synthetic GH to elderly subjects in 1990, thereby
444 reversing a number of aging-associated effects such as expansion of adipose mass (Rudman et al. 1990).
445 This led to GH being celebrated as an anti-aging drug (Junnila et al. 2013), including dubious commercial
446 offers. Today's aging research, on the contrary, strongly assumes that the enhanced activity of the
447 GH/IGF1 axis accelerates aging and that its suppression could extend lifespan even in humans (Lopez-
448 Otin et al. 2013; Longo et al. 2015; Pitt and Kaeberlein 2015). In addition to several studies of synthetic
449 GH in humans yielding less convincing results than those of Rudman *et al*., the main reasons for this turn
450 are the results of studies on short-lived model organisms. From worms to mice, the impairment of the
451 GH/IGF1 axis by genetic intervention consistently led to longer lifespans (Table 2), e.g., the up-regulation
452 of Klotho - an IGF1 inhibitor - extended the mouse lifespan by as much as 30 % (Kurosu et al. 2005). As
453 with the impairment of the GH/IGF1 axis, reducing of protein synthesis by decreasing the expression of
454 MYC, a basal transcription factor, extended the mouse lifespan by as much as 20 % (Hofmann et al.
455 2015) whereas the impairment of the respiratory chain by rotenone resulted in prolongation of the
456 killifish lifespan by 15 % (Baumgart et al. 2016) (Table 2).

457 Therefore, it is astonishing that massive up-regulation of these anabolic key components accompanies a
458 lifespan extension of approximately 100 % in long-lived mammals and potentially even contributes to it.
459 Several points could help to resolve this apparent contradiction: First, the up-regulation of anabolic
460 pathways and key genes is at least partially accompanied by the regulation of other mechanisms that
461 could plausibly compensate for deleterious effects. For example, it is, widely assumed that the negative
462 impact of enhanced protein synthesis on lifespan is to a large extent caused by the accumulation of
463 damaged or misfolded proteins, that is also known to contribute to aging-associated neurodegenerative
464 diseases (Hipkiss 2007; Saez and Vilchez 2014; Carmona and Michan 2016). Up-regulation of the
465 proteasome, as we observed in breeders in a weighted cross-tissue approach and especially in endocrine
466 tissues, is known to counteract these effects by clearing damaged proteins leading to lifespan extension
467 in worm and fly (Saez and Vilchez 2014). Enhanced proteasome activity has also been linked with higher
468 longevity of the naked mole-rat compared to the laboratory mouse (Perez et al. 2009; Rodriguez et al.
469 2012) and in comparative approaches across several mammalian lineages (Pride et al. 2015). We
470 hypothesize that the simultaneously high anabolic synthesis and catabolic degradation of proteins will
471 lead to a higher protein turnover rate in breeders and, accompanied with that, a reduced accumulation
472 of damaged and misfolded proteins. Similarly, it seems plausible that the up-regulation of the
473 mitochondrial respiratory chain (oxidative phosphorylation) in breeders is compensated for by
474 simultaneous up-regulation of the reactive oxygen hallmark: the mitochondrial respiratory chain is the
475 main source of cellular ROS which can damage DNA, proteins and other cellular components (Balaban et
476 al. 2005; Starkov 2008); the reactive oxygen hallmark consists by definition of genes that are known to
477 be up-regulated in response to ROS treatments. Unsurprisingly, at least 25 % of these genes code for
478 typical antioxidant enzymes such as thioredoxin, superoxide dismutase, peroxiredoxin, or catalase that
479 can detoxify ROS. Furthermore, the known cancer promoting effects of an enhanced GH/IGF1 axis
480 (Junnila et al. 2013) could, to some extent, be compensated for by up-regulation of apoptosis and p53

481 signaling, because these are major mechanisms of cancer suppression (Bieging et al. 2014). More
482 generally, potential lifespan-extending effects of moderate up-regulation of both the GH/IGF1 axis and
483 ROS production can also be viewed in the light of the hormesis hypothesis (Ristow 2014), which
484 postulates that mild stressors can induce overall beneficial adaptive stress responses. In line with these
485 arguments, we found higher resting metabolic rates in breeders compared to non-breeders in *Fukomys*
486 *anselli* (Schielke et al. 2017), a species closely related to *F. micklemi*.

487

488 **Table 2.** Behavior of important aging-relevant genes and pathways in this study.

Gene/Pathway	Regulation in indicated direction and species can reduce lifespan	Regulation in indicated direction and species can extend lifespan	Differentially expressed in this study in indicated tissues and direction*	Gene/Pathway is expressed mainly in the following tissues
Growth hormone (*GH1*)	Mouse ↑[1]	Mouse ↓[2], Rat ↓[2]	Pituitary gland ↑	Pituitary gland
Insulin growth factor 1 (*IGF1*)	–	Mouse ↓[2]	Adrenal gland ↑, Ovary ↑	Liver, Ovary
IGF1-receptor (*IGF1R*)	–	Mouse ↓[1], Worm ↓[3], Fly ↓[3]	Adrenal gland ↓, Ovary ↓	Many
Klotho (*KL*)	Mouse ↓[3]	Mouse ↑[3], Worm ↑[3]	Ovary ↓	Endocrine tissue, Kidney
SIRT1	–	Mouse ↑[6], Worm ↑[7], Fly ↑[7]	–	All
MYC	–	Mouse ↓[8]	Thyroid ↑	All
mTOR	–	Mouse ↓[9], Worm↓[9], Fly ↓[9]	Adrenal gland ↓	All
PRKAA2 (AMPK)	–	Worm ↑[9]	–	Many
TP53	Mouse ↑[11], Fly ↑[11]	Worm ↓[11], Mouse ↑[11], Fly ↑[11]	–	All
SOD2	–	Worm ↓[10], Fly ↑[10]	–	All
FOXO3	Fly ↑[12]	–	Ovary ↓, Adrenal gland ↓	All
Protein synthesis	–	Mouse ↓[8], Worm ↓[9], Fly ↓[9]	Many ↑	All
Proteasome	–	Worm ↑[14], Fly ↑[14]	Gonads ↑, Adrenal gland ↑	All
Lysosome	–	Worm ↑[13]	–	All
Respiratory chain	–	Worm↓[15], Fly ↓[16], Killifish ↓[17]	Gonads ↑, Adrenal gland ↑, Blood ↑, Spleen ↑	All
Apoptosis	Mouse ↑[11], Fly ↑[11]	Worm ↓[11], Mouse ↑[11], Fly ↑[11]	Skin ↑, Pituitary gland ↑	All

1 (Junnila et al. 2013), 2 (Bartke 2019), 3 (van Heemst 2010), 4 (Elibol and Kilic 2018), 5 (Kwon et al. 2015), 6 (Satoh et al. 2013), 7 (Burnett et al. 2011), 8 (Hofmann et al. 2015), 9 (Johnson et al. 2013), 10 (Edrey and Salmon 2014), 11 (Feng et al. 2011), 12 (Giannakou et al. 2004), 13 (Carmona-Gutierrez et al. 2016), 14 (Saez and Vilchez 2014), 15 (Dillin et al. 2002), 16 (Copeland et al. 2009),17 (Baumgart et al. 2016)

*Direction: breeder/non-breeder

** Direction: old/young

– Either not affecting lifespan or not known to the best of our knowledge (column 1 and 2); no change (column 3)

A second point that could help to resolve this apparent contradiction concerns the time of intervention. The transition from non-breeder to breeder takes place in adulthood, when by far the largest portion of the growth process has already been completed. In contrast, genetic interventions aimed at prolonging the lifespan by inhibiting the GH/IGFH1 axis (Table 2) usually affect the organisms throughout their entire lifespan, including infancy and youth. Therefore, it is still under debate whether the up-regulation of translation and anabolic processes by the GH/IGF1 axis independently enhances growth and aging or enhances aging only secondarily as a consequence of accelerated growth (Bartke 2017). Our results are an argument for the latter.

A third point is the question of the transferability of knowledge obtained in one species to other species. Most insights into current aging research originate from very short-lived model organisms (Table 2). It is clear, on the other hand, that the observed effects of lifespan-prolonging interventions listed in Table 2 are by far the smallest in the model organisms with the relatively longest lifespans: mice and rats. Compared to most other mammals, however, even mice and rats are short-lived. Given their body weight and an often-used correlation between body weight and lifespan across mammals, their observed maximum lifespan of about four years corresponds to only 51 % (for mice) and 32 % (for rats) of the expected maximum lifespan. In contrast, humans can live as much as 463% as long as they would be expected based on their body weight. This disparity makes them, given this particular model, the most extreme known non-flying mammal species regarding maximum longevity residual (Tacutu et al.

516 2013). According to current data, *Fukomys* mole-rats reach values of ca. 200 % and thus can be regarded
517 to be closer to humans than to mice or rats in this respect. It is currently unclear to what degree aging
518 mechanisms and lifespan-affecting interventions that were discovered in short-lived model species
519 apply to organisms that are far more long-lived, as in our experiment (e.g. (Parker et al. 2004; Keller and
520 Jemielity 2006)). It seems reasonable to hypothesize that specific interventions that prolong the lifespan
521 of long-lived organisms may have no major effect in short-lived species, and vice versa. For example, it
522 could be that changes suitable to prolong the life of species with a low cancer-risk (e.g., African mole-
523 rats, blind mole rats) (Buffenstein 2008; Gorbunova et al. 2012; Delaney et al. 2013) would have no or
524 only a marginal effect in laboratory mice, whose primary cause of natural death is cancer (Seluanov et
525 al. 2018). Therefore, it may also be possible that those gene expression patterns caused by our lifespan-
526 extending intervention in *Fukomys* mole-rats but contradicting the current knowledge obtained from
527 short-lived organisms may highlight differences in aging mechanisms between short-lived and long-lived
528 species.

529 As a fourth perspective, one could interpret the down-regulation of the GH/IGF1 axis in non-breeders as
530 a byproduct of the apparent up-regulation of the HPA axis in non-breeders, that may well be adaptive in
531 itself. In the wild, non-breeding *Fukomys* mole-rats can maximize their inclusive fitness by either
532 supporting their kin in their natal family or by founding a new family elsewhere. It has therefore been
533 suggested that the shorter lives of non-breeders could be adaptive on the ultimate level if longevity
534 were traded against some other fitness traits, such as competitiveness, to defend colonies against
535 intruders or to enhance their chances for successful dispersal (Dammann and Burda 2006). A
536 constitutively more activated HPA stress axis is expected to offer advantages for both family defense
537 and dispersal but it carries the risk of status-specific aging symptoms, such as muscle weakness, lower
538 GH/IGF1 axis activity, lower bone density etc. in the long run (Ferrau and Korbonits 2015). This effect

539 may become even more pronounced under laboratory conditions where grown non-breeders cannot
540 decide to disperse even if they would like to.

541 However, even the down-regulation of the GH/IGF-axis may be adaptive in itself for non-breeders if it
542 has the potential to protect them from further damage. Note that for today's conventional view that
543 stronger activation of the GH/IGF1 axis accelerates aging (Table 2), it is generally challenging that
544 decreasing activity is well documented to correlate with chronological age in a wide range of mammals,
545 including mice, rats, dogs, and humans (Bartke 2019). Also, decreasing activity correlates, under
546 pathologic conditions such as Cushing's syndrome, with many symptoms akin to aging (Fig. 5). It has
547 been suggested that one solution to this apparent contradiction may be that that the GH/IGF1 axis is
548 adaptively down-regulated in aging organisms as a reaction to already accumulated aging-related
549 symptoms so that additional damage can be avoided (Berryman et al. 2008; Milman et al. 2016).

550 Finally, recent findings of positively selected genes in African mole-rats (family Bathyergidae, containing
551 also *Fukomys* and *Heterocephalus*) could partly explain some of the surprising results. It is striking that
552 translation, and oxidative phosphorylation were among the strongest differentially expressed molecular
553 processes concering the breeding status. Earlier, these processes were also reported to be the most
554 affected by positive selection in the phylogeny of African mole-rats (Sahm et al. 2018b). Furthermore,
555 *IGF1* was one of thirteen genes that were found to be under positive selection in the last common
556 ancestor of the mole-rats. This may indicate that the corresponding mechanisms were evolutionarily
557 adapted to be less detrimental and make their up-regulation more compatible with a long lifespan. Since
558 the mere fact of positive selection does not permit to draw conclusions about the direction of the
559 mechanistic effect, this hypothesis, however, needs to remain speculative.

560 ## Conclusions

561 We performed a comprehensive transcriptome analysis that, for the first time within mammalian
562 species, compared naturally occurring cohorts of species with massively diverging aging rates. The
563 comparison of faster-aging *Fukomys* non-breeders with similar animals that were experimentally
564 elevated to the slower-aging breeder status revealed by far the most robust transcriptome differences
565 within endocrine tissue: adrenal gland, ovary, thyroid, and pituitary gland. Genes and pathways involved
566 in anabolism, such as *GH*, *IGF1*, translation and oxidative phosphorylation, were differentially expressed.
567 Their inhibition is among the best-documented life-prolonging interventions in a wide range of short-
568 lived model organisms (Table 2). Surprisingly, however, we found that the expression of these
569 mechanisms was consistently higher in slower-aging breeders than in faster-aging non-breeders. This
570 indicates that even basic molecular mechanisms of the aging process known from short-lived species
571 cannot easily be transferred to long-lived species. In particular, this applies to the role of the GH/IGF1
572 axis, which has in recent years been unilaterally described as harmful (Lopez-Otin et al. 2013; Pitt and
573 Kaeberlein 2015; Bartke 2017). In addition, special features of the mole-rats could also contribute to the
574 explanation of the unexpected result that genes and processes differentially expressed between
575 reproductive statuses were also strongly altered during the evolution of the mole-rats (Sahm et al.
576 2018b). Another intriguing possibility is that, in line with the hormesis hypothesis (Ristow 2014),
577 moderate harmful effects of anabolic processes can be hyper-compensated for by up-regulation of
578 pathways such as proteasomes, P53-signaling and antioxidant defense against ROS that we observed in
579 slower-aging breeders as well.

580 Furthermore, our work provides evidence that the HPA stress axis is a key regulator for the observed
581 downstream effects, including the lifespan difference. The effects are likely to be triggered by
582 differential expression of the gene *MC2R* coding for the ACTH receptor resulting in an altered stress

583 response in breeders vs. non-breeders. This is supported by the fact that cortisol levels in the non-
584 breeders are elevated. Furthermore, the set of direct and indirect target genes of the glucocorticoid
585 receptors is strongly affected by differential expression, and numerous known downstream effects of
586 glucocorticoid excess have been demonstrated for non-breeders, such as muscle weakness, weight gain,
587 and GH/IGF1 axis impairment. Overall, this evidence suggests that *MC2R* and other genes along the
588 described signalling pathway are promising targets for possible interventions in aging research.

589 # Methods

590 ## Animal care and sampling

591 All animals were housed in glass terraria with dimensions adjusted to the size of the family (min. 40 cm ×
592 60 cm) in the Department of General Zoology, Faculty of Biosciences, University of Duisburg-Essen. The
593 terraria are filled with a 5 cm layer of horticultural peat or sawdust. Tissue paper strips, tubes, and solid
594 shelters were provided as bedding/nesting materials and environmental enrichment. Potatoes and
595 carrots are supplied ad libitum as stable food, supplemented with apples, lettuce, and cereals. *Fukomys*
596 mole-rats do not drink free water. Temperature was kept fairly constant at 26± 1 °C, and humidity, at
597 approximately 40 %. The daily rhythm was set to 12 hours darkness and 12 hours light.

598 New breeder pairs (new families) were established between March and May 2014. Each new family was
599 founded by two unfamiliar, randomly chosen adult non-breeders of similar age (min/max/mean:
600 1.56/6.5/3.58 years in *F. mechowii*; 1.8/5.4/3.1 years in *F. micklemi*) and opposite sex and were taken
601 from already existing separate colonies. These founder animals were moved to a new terrarium in
602 which they were permanently mated. In both species, more than 80 % of these new pairs reproduced
603 within the first 12 months (total number of offspring by the end of the year 2016, 82 *F. micklemi* and 81
604 *F. mechowii*). Only founders with offspring were subsequently assigned to the breeder cohort; founders

605 without offspring were excluded from the study. Non-breeders remained in their natal family together
606 with both parents and other siblings.

607 *F. mechowii* were sampled in five distinct sampling sessions between March 2015 and winter
608 2016/2017. F. *micklemi* were sampled in three distinct sampling sessions between November 2016 and
609 July 2017. In both species, females were killed 4 to 6 months later than their male mates to ensure that
610 these breeder females were neither pregnant nor lactating at the time of sampling, in order to exclude
611 additional uncontrolled variables.

612 Before sampling, animals were anaesthetized with 6 mg/kg ketamine combined with 2.5 mg/kg xylazine
613 (Garcia Montero et al. 2015). Once the animals lost their pedal withdrawal reflex, 1 to 2 ml of blood was
614 collected by cardiac puncture, and the animals were killed by surgical decapitation. Blood samples (100
615 µl) were collected in RNAprotect Animal Blood reagent (Qiagen, Venlo, Netherlands). Tissue samples –
616 hippocampus, hypothalamus, pituitary gland, thyroid, heart, skeletal muscle (M. quadriceps femoris),
617 lateral skin, small intestine (ileum), upper colon, spleen, liver, kidney, adrenal gland, testis, and ovary –
618 were transferred to RNAlater (Qiagen, Venlo, Netherlands) immediately after dissection and, following
619 incubation, were stored at -80°C until analysis.

620 Animal housing and tissue collection were compliant with national and state legislation (breeding
621 allowances 32-2-1180-71/328 and 32-2-11-80-71/345; ethics/animal experimentation approval 84–
622 02.04.2013/A164, Landesamt für Natur-, Umwelt- und Verbraucherschutz Nordrhein-Westfalen).

623 RNA preparation and sequencing

624 For all tissues except blood, RNA was purified with the RNeasy Mini Kit (Qiagen) according to the
625 manufacturer's protocol. Blood RNA was purified with the RNeasy Protect Animal Blood Kit (Qiagen).
626 Kidney and heart samples were treated with proteinase K before extraction, as recommended by the

627 manufacturer. Library preparation was performed using the TruSeq RNA v2 kit (Illumina, San Diego, USA)
628 which includes selection of poly-adenylated RNA molecules. RNA-seq was performed by single-end
629 sequencing with 51 cycles in high-output mode on a HiSeq 2500 sequencing system (Illumina) and with
630 at least 20 million reads per sample, as described in Table S9. Read data for *F. mechowii* and *F. micklemi*
631 were deposited as European Nucleotide Archive study with the ID PRJEB29798 (Table S9).

632 Read mapping and quantification

633 It was ensured for all samples that the results of the respective sequencing passed "per base" and "per
634 sequence" quality checks of FASTQC (Andrews). The reads were then mapped against previously
635 published and with human gene symbols annotated *F. mechowii* and *F. micklemi* transcriptome data
636 (Sahm et al. 2018a; Sahm et al. 2018b). For both species, only the longest transcript isoform per gene
637 was used; this is the method of choice for selecting a representative variant in large-scale experiments
638 (Ezkurdia et al. 2015) (Data S2, S3). This selection resulted in 15,864 reference transcripts (genes) for *F.*
639 *mechowii* and in 16,400 for *F. micklemi*. After mapping and quantification, we further analyzed only
640 those reference transcripts whose gene symbols were present in the transcript catalogs of both species
641 – this was the case for 15,199 transcripts (the size of the union was 17,065). As mapping algorithm "bwa
642 aln" of the Burrows-Wheeler Aligner (BWA) (Li and Durbin 2009) was used, allowing no gaps and a
643 maximum of two mismatches in the alignment. Only those reads that could be uniquely mapped to the
644 respective gene were used for quantification. Read counts per gene and sample can be found in Data S4.
645 As another check, we ensured that all samples exhibited a Pearson correlation coefficient of at least 90%
646 in a pairwise comparison based on $\log_2$-transformed read counts against all other samples of the same
647 experimental group as defined by samples that were equal in the tissue as well as the species, sex, and
648 reproductive status of the source animal.

Differentially expressed genes analysis

P-values for differential gene expression and fold-changes were determined with DESeq2 (Love et al. 2014) and a multi-factorial design. The DESeq2-algorithm also includes strict filtering based on a normalized mean gene count that makes further pre-filtering unnecessary (Love et al. 2014). Therefore, those genes whose read count was zero for all examined samples were removed before further analysis, thereby reducing the number of analyzed genes to 15,181. The multi-factorial design means that, separately for each tissue, we input the read count data of samples across species, sex, and reproductive status into DESeq2 for each sample. This allowed DESeq2 to perform DEG-analysis between the two possible states of each of the variables by controlling for additional variance in the other two variables. This approach resulted in a four-times higher sample size than with an approach that would have been based on comparisons of two experimental groups, each of which would be equal in tissue, species, sex, and reproductive status. It is known that the statistical power in RNA-seq experiments can increase considerably with sample size (Ching et al. 2014). P-values were corrected for multiple testing with the Benjamini-Hochberg correction (Benjamini and Y. 1995) (false discovery rate – FDR).

The results of the DEG-analysis can be found in Data S5-S7.

Enrichment analysis on pathway and cross-tissue level

Let $(p_1^t, \dots p_n^t)$ represent the p-values obtained from differential gene expression analysis in the tissue corresponding with index t and the indices $1, \dots, n$ corresponding to the examined genes. Furthermore, let $(p_{x_1}^t, \dots., p_{x_m}^t)$, with $1 \leq x_i \leq n$ and $1 \leq i \leq m$, represent the p-values of genes with the indices $X = (x_1, \dots, x_m)$ belonging to a corresponding pathway that is tested for enrichment of differential expression signals. To determine the enrichment p-values at the pathway-level, we calculated the test statistic $\mathcal{F}_X^t$ for the gene indices X in tissue index t according to Fisher's method for combining p-values also known as Brown's method:

$$\mathcal{F}_X^t = -2 * \sum_{i=1}^{m} \log_e (p_{x_i}^t)$$

Because p-values at the gene level were, as is common in RNA-seq experiments (Väremo et al. 2013), not equally distributed, we empirically estimated the null distribution of the test statistic for each pathway instead of using the χ^2-distribution as frequently suggested in the literature (Fridley et al. 2010; Evangelou et al. 2012; Poole et al. 2016). This was done by calculating $\mathcal{F}_{X^j}^t$ for 1,000 random drawings, each without replacement, $X^j = (x_1^j, \dots, x_m^j)$, with $1 \leq x_k^j \leq n,\ 1 \leq j \leq 1000$. If the resulting p-value was zero (meaning $\forall\ 1 \leq j \leq 1000$: $\mathcal{F}_X^t > F_{X^j}^t$), the procedure was repeated with 10,000 and 100,000 random drawings, respectively. In addition, the indices X were divided into X_{up} and X_{down}, depending on whether their fold-change was > 1 or < 1 in breeder vs. non-breeder comparison, and $\mathcal{F}_{X_{up}}^t$ and $\mathcal{F}_{X_{down}}^t$ calculated. The ratio $\frac{\mathcal{F}_{X_{up}}^t}{\mathcal{F}_{X_{down}}^t}$ was used as an indicator for functional up- or down-regulation of the corresponding pathway (Fig. 4, Fig. S3, S4). Using this approach, enrichment p-values were estimated for all KEGG-pathways (Kanehisa et al. 2017) and MSigDB-hallmarks (Liberzon et al. 2015), as well as across all examined tissues (Data S8, S9). In addition, the procedure was applied to test whether the known 300 direct and 1300 indirect glucocorticoid receptor target genes (Phuc Le et al. 2005) were enriched for status-dependent differential expression signals (Tables S7, S8).

Similarly, cross-tissue DEG-p-values were weighted with a modified test statistic (c.f. (Heard and Rubin-Delanchy 2018)). Given the definitions from above, we calculated the weighted cross-tissue test statistic $\mathcal{F}^g$ for the gene g as follows:

$$\mathcal{F}^g = |2 * \sum_{t=1}^{l} (\log_e(p_g^t) * w_g^t)|$$

691 $$\text{with } w_g^t = \frac{\overline{expr}_g^t * sgn(logFC_g^t)}{\sum_{t=1}^{l} \overline{expr}_g^t}$$

692 where $logFC_g^t$ and $\overline{expr}_g^t$ are the logarithmized fold-change between reproductive states and
693 normalized mean expression (across sexes, species, and reproductive status) for the gene with index g
694 and tissue with index t – both calculated by DESeq2 (Love et al. 2014) –, sgn is the signum function, and
695 l is the number of examined tissues. The reasoning for using this test statistic was as follows: For the
696 weighted cross-tissue analysis, we assumed that the gene serves the same function throughout the
697 entire organism. Therefore, the test statistic given above weights the p-values of the various tissues by
698 the respective expression levels in those tissues. This ensures that, weighting e. g., a ubiquitously
699 expressed genes such as *TP53* is relatively equally across tissues, whereas for typical steroid hormone-
700 biosynthesis genes, such as *CYP11A1*, the endocrine tissue results determine almost exclusively the
701 weighted cross-tissue p-value. Furthermore, the test statistic rewards, based on the mentioned
702 assumption, consistency in the direction of gene regulation throughout tissues. All calculated values for
703 $logFC_g^t$, $\overline{expr}_g^t$, p_g^t, as well as the resulting $\mathcal{F}^g$ and p-values, can be found in Data S10.

704 Finally, weighted cross-tissue enrichment p-values at the pathway level were estimated by applying the
705 above-described method at the pathway level (based on test statistic $\mathcal{F}$) to the gene level weighted
706 cross-tissue p-values.

707 P-values were corrected for multiple testing with the Benjamini-Hochberg correction (Benjamini and Y.
708 1995) (FDR).

709 Weighted gene co-expression network analysis

710 We used the WGCNA R package to perform weighted correlation network analysis (Langfelder and
711 Horvath 2008) of all 636 samples at once. We followed the authors' usage recommendation by choosing
712 a soft power threshold based on scale-free topology and mean connectivity development (we chose

713 power=26 with a soft R^2 of 0.92 and a mean connectivity of 38.6), using biweight midcorrelation, setting
714 maxPOutliers to 0.1, and using "signed" both as network and topological overlap matrix type. The
715 maximum block size was chosen such that the analysis was performed with a single block and the
716 minimum module size was set to 30. The analysis divided the genes into 26 modules, of which 5 were
717 enriched for reproductive status DEGs based on Fisher's exact test and an FDR threshold of 0.05. Those
718 5 modules were tested for enrichment among KEGG-pathways (Kanehisa et al. 2017) with the same test
719 and significance threshold (Table S10). In addition, module eigengenes were determined and clustered
720 (Table S10). Then the topological overlap matrix that resulted from the WGCNA analysis ($TOM =$
721 $[tom_{i,j}]$, where the row indices $1 \leq i \leq |examined\ genes|$ correspond to genes and the column
722 indices $1 \leq j \leq |examined\ samples|$ correspond to samples) was used to determine pairwise
723 connectivity between all KEGG-pathways that showed differential expression at the weighted cross-
724 tissue level (Fig. S5). Based on the definition of connectivity of genes in a WGCNA analysis (Langfelder
725 and Horvath 2008), we defined the connectivity between two sets of indices X and Y each
726 corresponding to genes as $k_{X,Y} = \sum_{x \in X \setminus Y} \sum_{y \in Y \setminus X} tom_{x,y}$. P-values for the connectivities were
727 determined against null distributions that were empirically estimated by determining for each pair X
728 and Y the connectivities of 10,000 pairs of each $|X|$ and $|Y|$ randomly drawn indices (without
729 replacement), respectively. Since "signed" was used as the network and topological overlap matrix type,
730 the tests were one-sided.

731 Other analysis steps

732 Hierarchical clustering (Fig. S2) was performed based on Pearson correlation coefficients of $\log_2$-
733 transformed read counts between all sample pairs using the complete-linkage method (Defays 1977).
734 The principal variant component analysis (Fig. 2A) was performed with the pvca package from
735 Bioconductor (Bushel 2013) and a minimum demanded percentile value of the amount of the

736 variabilities, that the selected principal components needs to explain, of 0.5. Enrichments of DEGs
737 among genes enlisted in the Digital Aging Atlas database ((Craig et al. 2015), Data S11) were determined
738 with Fisher's exact test, the Benjamini-Hochberg method (FDR) (Benjamini and Y. 1995) for multiple test
739 correction, and a significance threshold of 0.05. Pathway visualization (Fig. S6-S9) was performed with
740 Pathview (Luo and Brouwer 2013). For the direction analysis of *Fukomys* reproductive status DEGs in
741 previous experiments in naked-mole rats and guinea pigs, we examined those 10 tissues that were
742 examined in all species (Table S6, Data S12). Separately for each tissue and combination of species –
743 naked mole-rat or guinea pig – and sex, we determined how many *Fukomys* reproductive status DEGs
744 were up-regulated or down-regulated. We also performed two-sided binomial tests on each of these
745 number pairs with a hypothesized success probability of 0.5. Furthermore, for each combination of
746 species and sex, two-sided exact binomial tests using 0.5 as parameter were performed based on the
747 sums of up-regulated and down-regulated genes across tissues (Table S6). For enrichment analysis of
748 direct and indirect glucocorticoid receptor target genes, mouse mRNA RefSeq IDs from Phuc Le et al.
749 (Phuc Le et al. 2005) were translated to human Entrez IDs and gene symbols via Ensembl Biomart (Data
750 S13). To statistically analyze the weight gain of the animals during the experiment, we used a type II
751 ANOVA with status, species, sex, and age as independent variables (Table S2); the weight gain, defined
752 as the difference in weights at beginning and the end of the experiment, as dependent variable (Fig. 6B);
753 and no interaction terms. If interaction terms were also used for the model, the p-value for the
754 difference in means between breeders and non-breeders changed from $7.49*10^{-3}$, as reported above, to
755 $7.46*10^{-6}$.

756 Bone density measurements

757 Frozen carcasses of all *F. micklemi* that had been part of the transcriptome study were scanned with a
758 self-shielded desktop small- animal computer tomography scanner (X-CUBE, Molecubes, Belgium). The

759 x-ray source was a tungsten anode (peak voltage, 50 kVp; tube current, 350 µA; 0.8 mm aluminum
760 filter). The detector was a cesium iodide (CsI) flat-panel, building up a screen with 1536 x 864 pixels.
761 Measurements were carried for individual 120 ms exposures, with angular sampling intervals of 940
762 exposures per rotation, for to a total of 7 rotations and a total exposure time of 789.6 seconds.

763 First, we first performed a calibration of the reconstructed CT data in terms of equivalent mineral
764 density. For this purpose, we used a bone density calibration phantom (BDC; QRM GmbH, Moehrendorf,
765 Germany) composed of five cylindrical inserts with a diameter of 5 mm containing various densities of
766 calcium hydroxyapatite (CaHA) surrounded by epoxy resin on a cylindrical shape. The nominal values of
767 CaHA were 0, 100, 200, 400, and 800 mg HA/cm^3, corresponding to a density of 1.13, 1.16, 1.25, 1.64,
768 and 1.90 g/cm^3 (certified with an accuracy of ± 0.5 %). The BDC was imaged and reconstructed with the
769 same specifications as each probe. From the reconstructed Hounsfield Units, a linear relationship was
770 determined against the known mineral concentrations.

771 Reconstruction of the acquired computer tomography data was carried with an Image Space
772 Reconstruction Algorithm, and spatial resolution was limited to the 100 µm voxel matrix reconstruction.
773 Spherical regions of interest (radius, 0.7 mm) were drawn on the sagittal plane of vertebrae T12, L1, and
774 L2. Care was taken to include all cancellous bone, excluding the cortical edges. Average Hounsfield Unit
775 values were computed on the calibration curve to finally retrieve equivalent densities of the regions of
776 interest.

777 Statistical analysis was performed using general linear models with bone density (Hounsfield Units) as
778 dependent variable, age (in days) as continuous covariate, and reproductive status and sex as nominal
779 cofactors. Models were calculated for each vertebra individually (individual models) and across all three
780 vertebrae (full model); in this latter case, vertebral number was added as additional categorial cofactor.

781 In all models, only main effects were calculated, no interactions. Analyses were performed with IBM
782 SPSS version 25 (Fig. 6C, Table S11).

783 Abbreviations

784 ANOVA – analysis of variance

785 ACTH – adrenocorticotropic hormone

786 DAA – Digital Aging Atlas

787 DEG – differentially expressed gene

788 DHEA – Dehydroepiandrosterone

789 FDR – false discovery rate

790 KEGG – Kyoto Encyclopedia of Genes and Genomes

791 MSigDB – Molecular Signatures Database

792 Data availability

793 Read datasets generated during the current study are available in the European Nucleotide Archive,
794 study ID: PRJEB29798.

795 Acknowledgments

796 We thank Ivonne Görlich, Christiane Vole, and Klaus Huse for excellent assistance in the preparation of
797 biological samples. We thank Konstantin Riege for fruitful discussions on the analysis of the data. We
798 thank Debra Weih and Flo Witte for proofreading the manuscript.

Funding

This work was funded by the Deutsche Forschungsgemeinschaft (DFG, PL 173/8-1 and DA 992/3-1; DFG Research Training Group 1739) and the Wiedenfeld-Stiftung/Stiftung Krebsforschung Duisburg. The funders had no role in study design, data collection and analysis, decision to publish, or preparation of the manuscript.

Authors' contributions

PD, MP, and KS conceived the project (with input from SB) and acquired the funding. PD, KS, and AS monitored the implementation of the project. PD, SB, HB, and PVD were responsible for housing the animals and implementing concrete mating schemes. PD, SB, ST, MGo, MS, JK, and PFC performed physiological measurements. PD, YH, KS, AS, SB, and MB sampled the animals. MG supervised library preparation and sequencing. AS, KS, and MB analyzed the data. AS, PD, MP, KS, SH, and PK interpreted the data and drafted the manuscript concept. All authors wrote and approved the manuscript.

Ethics declarations

The authors declare no competing interests.

Animal housing and tissue collection were compliant with national and state legislation (breeding allowances 32-2-1180-71/328 and 32-2-11-80-71/345, ethics/animal experimentation approval 84–02.04.2013/A164, Landesamt für Natur-, Umwelt- und Verbraucherschutz Nordrhein-Westfalen).

816 # Supplementary information

817 ## Supplement Figures

818 **Figure S1.** Overview of the tissues examined in this study with a schematic mole-rat representation.

819 **Figure S2.** Clustering of the 636 examined samples. Clustering was performed based on the Euclidian
820 distance of logarithmized pairwise Pearson read count correlations using the UPGMA method.

821 **Figure S3.** Full overview of Kyoto Encyclopedia of Genes and Genomes (KEGG) pathways that are
822 enriched for status-dependent differential gene expression.

823 **Figure S4.** Full overview of Molecular Signatures Database (MsigDB) hallmarks that are enriched for
824 status-dependent differential gene expression.

825 **Figure S5.** Pairwise connectivity of metabolic pathways that are enriched for status-dependent
826 differential gene expression at the cross-tissue level.

827 **Figure S6.** Status-dependent regulation of Kyoto Encyclopedia of Genes and Genomes (KEGG) pathway
828 hsa00140 Steroid hormone biosynthesis at the cross-tissue level.

829 **Figure S7.** Status-dependent regulation of Kyoto Encyclopedia of Genes and Genomes (KEGG) pathway
830 hsa05016 Huntington's disease at the cross-tissue level.

831 **Figure S8.** Status-dependent regulation of Kyoto Encyclopedia of Genes and Genomes (KEGG) pathway
832 hsa05012 Parkinson's disease at the cross-tissue level.

833 **Figure S9.** Status-dependent regulation of Kyoto Encyclopedia of Genes and Genomes (KEGG) pathway
834 hsa050160 Alzheimer's disease at the cross-tissue level.

835 ## Supplement Tables

836 **Table S1.** Overview of number of samples that were examined with regard to status, sex, species, and
837 tissue.

838 **Table S2.** Animal description.

839 **Table S3.** Overview of the tissues that were successfully sampled for each type of animal.

840 **Table S4.** Pairing scheme: *F. mechowii*.

841 **Table S5.** Pairing scheme: *F. micklemi*.

842 **Table S6.** Analysis of the direction of status-dependent differentially expressed genes that were
843 identified in this study (two *Fukomys* species) in similar experiments with naked mole-rats and guinea
844 pigs (Bens et al. 2018, https://www.ncbi.nlm.nih.gov/pmc/articles/PMC6090939/).

845 **Table S7.** Analysis of status-dependent differential gene expression enrichment on glucocorticoid
846 receptor target genes that were determined by Phuc Le at al. 2005
847 (https://www.ncbi.nlm.nih.gov/pmc/articles/PMC1186734/), using chromatin immunoprecipitation
848 (CHIP).

849 **Table S8.** Analysis of status-dependent differential gene expression enrichment on glucocorticoid
850 receptor target genes that were determined by Phuc Le at al. 2005
851 (https://www.ncbi.nlm.nih.gov/pmc/articles/PMC1186734/), using a differential gene expression
852 analysis.

853 **Table S9.** Sample description.

854 **Table S10.** WGCNA module clustering and functional enrichment analysis regarding these modules.

855 **Table S11.** Bone density measurements.

856 ## Supplement Data

857 **Data S1.** (zip) For each KEGG pathway and MSigDB hallmark that was detected to be significantly (FDR <
858 0.1) enriched for status-dependent differential expression at the weighted cross-tissue level, the data
859 set contains a *.tsv file with the genes that form the respective pathway/hallmark sorted by their
860 individual contribution to the enrichment. The files also provide an overview of the p-values and fold-
861 changes of those genes in those tissues in which the genes are expressed most highly.

862 **Data S2.** (fa.gz) Transcript isoforms of *F. mechowii* used for read mapping.

863 **Data S3.** (fa.gz) Transcript isoforms of *F. micklemi* used for read mapping.

864 **Data S4.** (tsv.gz) Raw read counts for all 17,065 genes and 636 samples that were analyzed in this study
865 using RNA-seq.

866 **Data S5.** (zip) DESeq2 results for status-dependent gene expression (direction: breeder/non-breeder).
867 The data set contains one *.tsv file per analyzed tissue.

868 **Data S6.** (zip) DESeq2 results for sex-dependent gene expression (direction: female/male). The data set
869 contains one *.tsv file per analyzed tissue.

870 **Data S7.** (zip) DESeq2 results for species-dependent gene expression (direction: mechowii/micklemi).
871 The data set contains one *.tsv file per analyzed tissue.

872 **Data S8.** (zip) Enrichment analysis results for status-dependent gene expression on KEGG pathways. The
873 data set contains one *.tsv file per analyzed tissue, as well as an additional *.tsv file for the weighted
874 cross-tissue level results.

875 **Data S9.** (zip) Enrichment analysis results for status-dependent gene expression on MSigDB hallmarks.
876 The data set contains one *.tsv file per analyzed tissue, as well as an additional *.tsv file for the
877 weighted cross-tissue level results.

878 **Data S10.** (tsv.gz) Overview of the weighted cross-tissue differential gene expression analysis. Contains
879 all p-values, fold-changes, and mean expression values for all genes across all tissues as well as the
880 weighted, combined cross-tissue test statistics, p-values, and fold-changes for all genes.

881 **Data S11.** (tsv) Genes of the Digital Aging Atlas used in this study.

882 **Data S12.** (zip) Comparison of status-dependent differentially expressed genes with results of an earlier,
883 similar study involving naked mole-rats (NMRs) and guinea pigs (GPs). The data set contains one *.tsv
884 file for each of the ten tissues that were examined in both studies. Each *.tsv file lists the differentially
885 expressed genes for the respective tissue as identified in this study with the determined FDRs and fold-
886 changes, as well as the fold-changes determined in the earlier study using naked mole-rats and guinea
887 pigs.

888 **Data S13**. (zip) Glucocorticoid receptor target genes that were determined by Phuc Le *et al.* and tested
889 in this study for enrichment of status-dependent differential gene expression. The data set contains one
890 *.tsv file each for target genes determined via chromatin immunoprecipitation (CHIP) and differential
891 gene expression analysis. Phuc Le et al. determined differentially expressed genes between mice that
892 were treated with exogenous glucocorticoids and untreated controls. The relevant table columns from
893 Phuc Le et al. were added by human gene symbol and Entrez IDs that were used for enrichment analysis.

894 # References

895 Allolio B, Arlt W. 2002. DHEA treatment: myth or reality? *Trends in Endocrinology & Metabolism* **13**: 288-
896 294.

897 Andrews S. FastQC A Quality Control tool for High Throughput Sequence Data.
898 http://wwwbioinformaticsbabrahamacuk/projects/fastqc/ doi:citeulike-article-id:11583827.
899 Annibaldi A, Meier P. 2018. Checkpoints in TNF-Induced Cell Death: Implications in Inflammation and
900 Cancer. *Trends Mol Med* **24**: 49-65.
901 Austad SN. 2009. Comparative biology of aging. *J Gerontol A Biol Sci Med Sci* **64**: 199-201.
902 Austad SN. 2011. Candidate bird species for use in aging research. *ILAR J* **52**: 89-96.
903 Baig S, Seevasant I, Mohamad J, Mukheem A, Huri HZ, Kamarul T. 2016. Potential of apoptotic pathway-
904 targeted cancer therapeutic research: Where do we stand? *Cell Death Dis* **7**: e2058.
905 Balaban RS, Nemoto S, Finkel T. 2005. Mitochondria, oxidants, and aging. *Cell* **120**: 483-495.
906 Bartke A. 2017. Somatic growth, aging, and longevity. *NPJ Aging Mech Dis* **3**: 14.
907 Bartke A. 2019. Growth Hormone and Aging: Updated Review. *World J Mens Health* **37**: 19-30.
908 Baulieu EE. 1996. Dehydroepiandrosterone (DHEA): a fountain of youth? *J Clin Endocrinol Metab* **81**:
909 3147-3151.
910 Baumgart M, Priebe S, Groth M, Hartmann N, Menzel U, Pandolfini L, Koch P, Felder M, Ristow M,
911 Englert C et al. 2016. Longitudinal RNA-Seq Analysis of Vertebrate Aging Identifies Mitochondrial
912 Complex I as a Small-Molecule-Sensitive Modifier of Lifespan. *Cell Syst* **2**: 122-132.
913 Becker DE. 2013. Basic and clinical pharmacology of glucocorticosteroids. *Anesth Prog* **60**: 25-31; quiz
914 32.
915 Benayoun BA, Pollina EA, Singh PP, Mahmoudi S, Harel I, Casey KM, Dulken BW, Kundaje A, Brunet A.
916 2019. Remodeling of epigenome and transcriptome landscapes with aging in mice reveals
917 widespread induction of inflammatory responses. *Genome Res* **29**: 697-709.
918 Benjamini Y, Y. H. 1995. Controlling the false discovery rate: A practical and powerful approach to
919 multiple testing. *Journal of the Royal Statistical Society Series B (Methodological)* **57**: 289-300.
920 Bens M, Szafranski K, Holtze S, Sahm A, Groth M, Kestler HA, Hildebrandt TB, Platzer M. 2018. Naked
921 mole-rat transcriptome signatures of socially suppressed sexual maturation and links of
922 reproduction to aging. *BMC Biol* **16**: 77.
923 Berryman DE, Christiansen JS, Johannsson G, Thorner MO, Kopchick JJ. 2008. Role of the GH/IGF-1 axis in
924 lifespan and healthspan: lessons from animal models. *Growth Horm IGF Res* **18**: 455-471.
925 Beuschlein F, Fassnacht M, Klink A, Allolio B, Reincke M. 2001. ACTH-receptor expression, regulation and
926 role in adrenocortial tumor formation. *Eur J Endocrinol* **144**: 199-206.
927 Bieging KT, Mello SS, Attardi LD. 2014. Unravelling mechanisms of p53-mediated tumour suppression.
928 *Nat Rev Cancer* **14**: 359-370.
929 Bodart G, Goffinet L, Morrhaye G, Farhat K, de Saint-Hubert M, Debacq-Chainiaux F, Swine C, Geenen V,
930 Martens HJ. 2015. Somatotrope GHRH/GH/IGF-1 axis at the crossroads between
931 immunosenescence and frailty. *Ann N Y Acad Sci* **1351**: 61-67.
932 Buffenstein R. 2008. Negligible senescence in the longest living rodent, the naked mole-rat: insights
933 from a successfully aging species. *J Comp Physiol B* **178**: 439-445.
934 Burda H. 1995. Individual recognition and incest avoidance in eusocial common mole-rats rather than
935 reproductive suppression by parents. *Experientia* **51**: 411-413.
936 Burkhardt T, Schmidt NO, Vettorazzi E, Aberle J, Mengel M, Flitsch J. 2013. DHEA(S)--a novel marker in
937 Cushing's disease. *Acta Neurochir (Wien)* **155**: 479-484; discussion 484.
938 Burnett C, Valentini S, Cabreiro F, Goss M, Somogyvari M, Piper MD, Hoddinott M, Sutphin GL, Leko V,
939 McElwee JJ et al. 2011. Absence of effects of Sir2 overexpression on lifespan in C. elegans and
940 Drosophila. *Nature* **477**: 482-485.
941 Bushel P. 2013. pvca: Principal Variance Component Analysis (PVCA).
942 Cannata D, Vijayakumar A, Fierz Y, LeRoith D. 2010. The GH/IGF-1 axis in growth and development: new
943 insights derived from animal models. *Adv Pediatr* **57**: 331-351.

944 Carmona-Gutierrez D, Hughes AL, Madeo F, Ruckenstuhl C. 2016. The crucial impact of lysosomes in
945 aging and longevity. *Ageing Res Rev* **32**: 2-12.
946 Carmona JJ, Michan S. 2016. Biology of Healthy Aging and Longevity. *Rev Invest Clin* **68**: 7-16.
947 Carotti S, Guarino MPL, Valentini F, Porzio S, Vespasiani-Gentilucci U, Perrone G, Zingariello M, Gallo P,
948 Cicala M, Picardi A et al. 2018. Impairment of GH/IGF-1 Axis in the Liver of Patients with HCV-
949 Related Chronic Hepatitis. *Horm Metab Res* **50**: 145-151.
950 Celec P, Starka L. 2003. Dehydroepiandrosterone - is the fountain of youth drying out? *Physiol Res* **52**:
951 397-407.
952 Chabre O. 2014. [Cushing syndrome: Physiopathology, etiology and principles of therapy]. *Presse Med*
953 **43**: 376-392.
954 Chahal HS, Drake WM. 2007. The endocrine system and ageing. *J Pathol* **211**: 173-180.
955 Ching T, Huang S, Garmire LX. 2014. Power analysis and sample size estimation for RNA-Seq differential
956 expression. *RNA* **20**: 1684-1696.
957 Copeland JM, Cho J, Lo T, Jr., Hur JH, Bahadorani S, Arabyan T, Rabie J, Soh J, Walker DW. 2009.
958 Extension of Drosophila life span by RNAi of the mitochondrial respiratory chain. *Curr Biol* **19**:
959 1591-1598.
960 Craig T, Smelick C, Tacutu R, Wuttke D, Wood SH, Stanley H, Janssens G, Savitskaya E, Moskalev A, Arking
961 R et al. 2015. The Digital Ageing Atlas: integrating the diversity of age-related changes into a
962 unified resource. *Nucleic Acids Res* **43**: D873-878.
963 Dammann P. 2017. Slow aging in mammals-Lessons from African mole-rats and bats. *Semin Cell Dev Biol*
964 **70**: 154-163.
965 Dammann P, Burda H. 2006. Sexual activity and reproduction delay ageing in a mammal. *Curr Biol* **16**:
966 R117-118.
967 Dammann P, Scherag A, Zak N, Szafranski K, Holtze S, Begall S, Burda H, Kestler HA, Hildebrandt T,
968 Platzer M. 2019. Comment on 'Naked mole-rat mortality rates defy Gompertzian laws by not
969 increasing with age'. *Elife* **8**.
970 Dammann P, Sell DR, Begall S, Strauch C, Monnier VM. 2012. Advanced glycation end-products as
971 markers of aging and longevity in the long-lived Ansell's mole-rat (Fukomys anselli). *J Gerontol A*
972 *Biol Sci Med Sci* **67**: 573-583.
973 Dammann P, Sumbera R, Massmann C, Scherag A, Burda H. 2011. Extended longevity of reproductives
974 appears to be common in Fukomys mole-rats (Rodentia, Bathyergidae). *PLoS One* **6**: e18757.
975 Defays D. 1977. An efficient algorithm for a complete link method. *The Computer Journal* **20**: 364-366.
976 Delaney MA, Nagy L, Kinsel MJ, Treuting PM. 2013. Spontaneous histologic lesions of the adult naked
977 mole rat (Heterocephalus glaber): a retrospective survey of lesions in a zoo population. *Vet*
978 *Pathol* **50**: 607-621.
979 Dillin A, Hsu AL, Arantes-Oliveira N, Lehrer-Graiwer J, Hsin H, Fraser AG, Kamath RS, Ahringer J, Kenyon
980 C. 2002. Rates of behavior and aging specified by mitochondrial function during development.
981 *Science* **298**: 2398-2401.
982 Edrey YH, Salmon AB. 2014. Revisiting an age-old question regarding oxidative stress. *Free Radic Biol*
983 *Med* **71**: 368-378.
984 Elibol B, Kilic U. 2018. High Levels of SIRT1 Expression as a Protective Mechanism Against Disease-
985 Related Conditions. *Front Endocrinol (Lausanne)* **9**: 614.
986 Etxabe J, Vazquez JA. 1994. Morbidity and mortality in Cushing's disease: an epidemiological approach.
987 *Clin Endocrinol (Oxf)* **40**: 479-484.
988 Evangelou M, Rendon A, Ouwehand WH, Wernisch L, Dudbridge F. 2012. Comparison of Methods for
989 Competitive Tests of Pathway Analysis. *PLOS ONE* **7**: e41018.

990 Ezkurdia I, Rodriguez JM, Carrillo-de Santa Pau E, Vazquez J, Valencia A, Tress ML. 2015. Most highly
991 expressed protein-coding genes have a single dominant isoform. *J Proteome Res* **14**: 1880-1887.
992 Feng Z, Lin M, Wu R. 2011. The Regulation of Aging and Longevity: A New and Complex Role of p53.
993 *Genes Cancer* **2**: 443-452.
994 Ferrau F, Korbonits M. 2015. Metabolic comorbidities in Cushing's syndrome. *Eur J Endocrinol* **173**:
995 M133-157.
996 Fridley BL, Jenkins GD, Biernacka JM. 2010. Self-contained gene-set analysis of expression data: an
997 evaluation of existing and novel methods. *PloS one* **5**: e12693.
998 Fridmanis D, Roga A, Klovins J. 2017. ACTH Receptor (MC2R) Specificity: What Do We Know About
999 Underlying Molecular Mechanisms? *Front Endocrinol (Lausanne)* **8**: 13.
1000 Garcia Montero A, Burda H, Begall S. 2015. Chemical restraint of African mole-rats (Fukomys sp.) with a
1001 combination of ketamine and xylazine. *Vet Anaesth Analg* **42**: 187-191.
1002 Giannakou ME, Goss M, Junger MA, Hafen E, Leevers SJ, Partridge L. 2004. Long-lived Drosophila with
1003 overexpressed dFOXO in adult fat body. *Science* **305**: 361.
1004 Gjerstad JK, Lightman SL, Spiga F. 2018. Role of glucocorticoid negative feedback in the regulation of
1005 HPA axis pulsatility. *Stress* **21**: 403-416.
1006 Gorbunova V, Hine C, Tian X, Ablaeva J, Gudkov AV, Nevo E, Seluanov A. 2012. Cancer resistance in the
1007 blind mole rat is mediated by concerted necrotic cell death mechanism. *Proc Natl Acad Sci U S A*
1008 **109**: 19392-19396.
1009 Hammer F, Subtil S, Lux P, Maser-Gluth C, Stewart PM, Allolio B, Arlt W. 2005. No Evidence for Hepatic
1010 Conversion of Dehydroepiandrosterone (DHEA) Sulfate to DHEA: In Vivo and in Vitro Studies.
1011 *The Journal of Clinical Endocrinology & Metabolism* **90**: 3600-3605.
1012 Hands SL, Proud CG, Wyttenbach A. 2009. mTOR's role in ageing: protein synthesis or autophagy? *Aging*
1013 *(Albany NY)* **1**: 586-597.
1014 Harman D. 1956. Aging: a theory based on free radical and radiation chemistry. *J Gerontol* **11**: 298-300.
1015 Harman D. 2001. Aging: overview. *Ann N Y Acad Sci* **928**: 1-21.
1016 Heard NA, Rubin-Delanchy P. 2018. Choosing between methods of combining p-values. *Biometrika*
1017 **105**: 239-246.
1018 Henning Y, Vole C, Begall S, Bens M, Broecker-Preuss M, Sahm A, Szafranski K, Burda H, Dammann P.
1019 2014. Unusual ratio between free thyroxine and free triiodothyronine in a long-lived mole-rat
1020 species with bimodal ageing. *PLoS One* **9**: e113698.
1021 Hipkiss AR. 2007. On why decreasing protein synthesis can increase lifespan. *Mech Ageing Dev* **128**: 412-
1022 414.
1023 Hofmann JW, Zhao X, De Cecco M, Peterson AL, Pagliaroli L, Manivannan J, Hubbard GB, Ikeno Y, Zhang
1024 Y, Feng B et al. 2015. Reduced expression of MYC increases longevity and enhances healthspan.
1025 *Cell* **160**: 477-488.
1026 Imai T, Sarkar D, Shibata A, Funahashi H, Morita-Matsuyama T, Kikumori T, Ohmori S, Seo H. 2001.
1027 Expression of adrenocorticotropin receptor gene in adrenocortical adenomas from patients with
1028 Cushing syndrome: possible contribution for the autonomous production of cortisol. *Ann Surg*
1029 **234**: 85-91.
1030 Jarvis JU, Bennett NC. 1993. Eusociality has evolved independently in two genera of bathyergid mole-
1031 rats — but occurs in no other subterranean mammal. *Behavioral Ecology and Sociobiology* **33**:
1032 253-260.
1033 Johnson SC, Rabinovitch PS, Kaeberlein M. 2013. mTOR is a key modulator of ageing and age-related
1034 disease. *Nature* **493**: 338-345.
1035 Jones CM, Boelaert K. 2015. The Endocrinology of Ageing: A Mini-Review. *Gerontology* **61**: 291-300.
1036 Jung HJ, Suh Y. 2014. Regulation of IGF -1 signaling by microRNAs. *Front Genet* **5**: 472.

1037 Junnila RK, List EO, Berryman DE, Murrey JW, Kopchick JJ. 2013. The GH/IGF-1 axis in ageing and
1038 longevity. *Nat Rev Endocrinol* **9**: 366-376.
1039 Kanehisa M, Furumichi M, Tanabe M, Sato Y, Morishima K. 2017. KEGG: new perspectives on genomes,
1040 pathways, diseases and drugs. *Nucleic Acids Res* **45**: D353-D361.
1041 Keller L, Jemielity S. 2006. Social insects as a model to study the molecular basis of ageing. *Exp Gerontol*
1042 **41**: 553-556.
1043 Kooistra HS, Galac S. 2012. Recent Advances in the Diagnosis of Cushing's Syndrome in Dogs. *Topics in*
1044 *Companion Animal Medicine* **27**: 21-24.
1045 Kurosu H, Yamamoto M, Clark JD, Pastor JV, Nandi A, Gurnani P, McGuinness OP, Chikuda H, Yamaguchi
1046 M, Kawaguchi H et al. 2005. Suppression of aging in mice by the hormone Klotho. *Science* **309**:
1047 1829-1833.
1048 Kwon Y, Kim J, Lee CY, Kim H. 2015. Expression of SIRT1 and SIRT3 varies according to age in mice. *Anat*
1049 *Cell Biol* **48**: 54-61.
1050 Langfelder P, Horvath S. 2008. WGCNA: an R package for weighted correlation network analysis. *BMC*
1051 *Bioinformatics* **9**: 559.
1052 Li H, Durbin R. 2009. Fast and accurate short read alignment with Burrows-Wheeler transform.
1053 *Bioinformatics* **25**: 1754-1760.
1054 Liberzon A, Birger C, Thorvaldsdottir H, Ghandi M, Mesirov JP, Tamayo P. 2015. The Molecular
1055 Signatures Database (MSigDB) hallmark gene set collection. *Cell Syst* **1**: 417-425.
1056 Lin L, Hindmarsh PC, Metherell LA, Alzyoud M, Al-Ali M, Brain CE, Clark AJ, Dattani MT, Achermann JC.
1057 2007. Severe loss-of-function mutations in the adrenocorticotropin receptor (ACTHR, MC2R) can
1058 be found in patients diagnosed with salt-losing adrenal hypoplasia. *Clin Endocrinol (Oxf)* **66**: 205-
1059 210.
1060 Liu D, Ahmet A, Ward L, Krishnamoorthy P, Mandelcorn ED, Leigh R, Brown JP, Cohen A, Kim H. 2013. A
1061 practical guide to the monitoring and management of the complications of systemic
1062 corticosteroid therapy. *Allergy Asthma Clin Immunol* **9**: 30.
1063 Liu Y, Ordovas JM, Gao G, Province M, Straka RJ, Tsai MY, Lai CQ, Zhang K, Borecki I, Hixson JE et al.
1064 2008. The SCARB1 gene is associated with lipid response to dietary and pharmacological
1065 interventions. *J Hum Genet* **53**: 709-717.
1066 Longo VD, Antebi A, Bartke A, Barzilai N, Brown-Borg HM, Caruso C, Curiel TJ, de Cabo R, Franceschi C,
1067 Gems D et al. 2015. Interventions to Slow Aging in Humans: Are We Ready? *Aging Cell* **14**: 497-
1068 510.
1069 Lopez-Otin C, Blasco MA, Partridge L, Serrano M, Kroemer G. 2013. The hallmarks of aging. *Cell* **153**:
1070 1194-1217.
1071 Love MI, Huber W, Anders S. 2014. Moderated estimation of fold change and dispersion for RNA-seq
1072 data with DESeq2. *Genome Biol* **15**: 550.
1073 Lowe G, Rumley A. 2014. The relevance of coagulation in cardiovascular disease: what do the
1074 biomarkers tell us? *Thromb Haemost* **112**: 860-867.
1075 Lozier NR, Kopchick JJ, de Lacalle S. 2018. Relative Contributions of Myostatin and the GH/IGF-1 Axis in
1076 Body Composition and Muscle Strength. *Front Physiol* **9**: 1418.
1077 Luo W, Brouwer C. 2013. Pathview: an R/Bioconductor package for pathway-based data integration and
1078 visualization. *Bioinformatics* **29**: 1830-1831.
1079 Maggio M, Lauretani F, Ceda GP, Bandinelli S, Ling SM, Metter EJ, Artoni A, Carassale L, Cazzato A,
1080 Ceresini G et al. 2007. Relationship between low levels of anabolic hormones and 6-year
1081 mortality in older men: the aging in the Chianti Area (InCHIANTI) study. *Arch Intern Med* **167**:
1082 2249-2254.
1083 McCue PM. 2002. Equine Cushing's disease. *Vet Clin North Am Equine Pract* **18**: 533-543, viii.

1084 Meijer JC, Lubberink AA, Gruys E. 1978. Cushing's syndrome due to adrenocortical adenoma in a cat.
1085 *Tijdschr Diergeneeskd* **103**: 1048-1051.
1086 Miller WL, Auchus RJ. 2011. The molecular biology, biochemistry, and physiology of human
1087 steroidogenesis and its disorders. *Endocr Rev* **32**: 81-151.
1088 Milman S, Huffman DM, Barzilai N. 2016. The Somatotropic Axis in Human Aging: Framework for the
1089 Current State of Knowledge and Future Research. *Cell Metab* **23**: 980-989.
1090 Morimoto RI, Cuervo AM. 2009. Protein homeostasis and aging: taking care of proteins from the cradle
1091 to the grave. *J Gerontol A Biol Sci Med Sci* **64**: 167-170.
1092 Newfield RS. 2010. ACTH receptor blockade: a novel approach to treat congenital adrenal hyperplasia, or
1093 Cushing's disease. *Med Hypotheses* **74**: 705-706.
1094 Ochi A, Adachi T, Inokuchi K, Ogawa K, Nakamura Y, Chiba Y, Kawasaki S, Onishi Y, Onuma Y, Munetsugu
1095 Y et al. 2016. Effects of Aging on the Coagulation Fibrinolytic System in Outpatients of the
1096 Cardiovascular Department. *Circ J* **80**: 2133-2140.
1097 Parker JD, Parker KM, Sohal BH, Sohal RS, Keller L. 2004. Decreased expression of Cu-Zn superoxide
1098 dismutase 1 in ants with extreme lifespan. *Proc Natl Acad Sci U S A* **101**: 3486-3489.
1099 Perez VI, Buffenstein R, Masamsetti V, Leonard S, Salmon AB, Mele J, Andziak B, Yang T, Edrey Y, Friguet
1100 B et al. 2009. Protein stability and resistance to oxidative stress are determinants of longevity in
1101 the longest-living rodent, the naked mole-rat. *Proc Natl Acad Sci U S A* **106**: 3059-3064.
1102 Phuc Le P, Friedman JR, Schug J, Brestelli JE, Parker JB, Bochkis IM, Kaestner KH. 2005. Glucocorticoid
1103 receptor-dependent gene regulatory networks. *PLoS Genet* **1**: e16.
1104 Pistritto G, Trisciuoglio D, Ceci C, Garufi A, D'Orazi G. 2016. Apoptosis as anticancer mechanism: function
1105 and dysfunction of its modulators and targeted therapeutic strategies. *Aging (Albany NY)* **8**: 603-
1106 619.
1107 Pitt JN, Kaeberlein M. 2015. Why is aging conserved and what can we do about it? *PLoS Biol* **13**:
1108 e1002131.
1109 Poole W, Gibbs DL, Shmulevich I, Bernard B, Knijnenburg TA. 2016. Combining dependent P-values with
1110 an empirical adaptation of Brown's method. *Bioinformatics (Oxford, England)* **32**: i430-i436.
1111 Pride H, Yu Z, Sunchu B, Mochnick J, Coles A, Zhang Y, Buffenstein R, Hornsby PJ, Austad SN, Perez VI.
1112 2015. Long-lived species have improved proteostasis compared to phylogenetically-related
1113 shorter-lived species. *Biochem Biophys Res Commun* **457**: 669-675.
1114 Raisingani M, Preneet B, Kohn B, Yakar S. 2017. Skeletal growth and bone mineral acquisition in type 1
1115 diabetic children; abnormalities of the GH/IGF-1 axis. *Growth Horm IGF Res* **34**: 13-21.
1116 Ristow M. 2014. Unraveling the truth about antioxidants: mitohormesis explains ROS-induced health
1117 benefits. *Nat Med* **20**: 709-711.
1118 Rodriguez KA, Edrey YH, Osmulski P, Gaczynska M, Buffenstein R. 2012. Altered Composition of Liver
1119 Proteasome Assemblies Contributes to Enhanced Proteasome Activity in the Exceptionally Long-
1120 Lived Naked Mole-Rat. *PLOS ONE* **7**: e35890.
1121 Ruby JG, Smith M, Buffenstein R. 2018. Naked Mole-Rat mortality rates defy gompertzian laws by not
1122 increasing with age. *Elife* **7**.
1123 Rudman D, Feller AG, Nagraj HS, Gergans GA, Lalitha PY, Goldberg AF, Schlenker RA, Cohn L, Rudman IW,
1124 Mattson DE. 1990. Effects of human growth hormone in men over 60 years old. *N Engl J Med*
1125 **323**: 1-6.
1126 Rutkowski K, Sowa P, Rutkowska-Talipska J, Kuryliszyn-Moskal A, Rutkowski R. 2014.
1127 Dehydroepiandrosterone (DHEA): hypes and hopes. *Drugs* **74**: 1195-1207.
1128 Saez I, Vilchez D. 2014. The Mechanistic Links Between Proteasome Activity, Aging and Age-related
1129 Diseases. *Curr Genomics* **15**: 38-51.

1130 Sahm A, Bens M, Henning Y, Vole C, Groth M, Schwab M, Hoffmann S, Platzer M, Szafranski K, Dammann
1131 P. 2018a. Higher gene expression stability during aging in long-lived giant mole-rats than in
1132 short-lived rats. *Aging (Albany NY)* **10**: 3938-3956.
1133 Sahm A, Bens M, Szafranski K, Holtze S, Groth M, Gorlach M, Calkhoven C, Muller C, Schwab M, Kraus J
1134 et al. 2018b. Long-lived rodents reveal signatures of positive selection in genes associated with
1135 lifespan. *PLoS Genet* **14**: e1007272.
1136 Salmon AB, Leonard S, Masamsetti V, Pierce A, Podlutsky AJ, Podlutskaya N, Richardson A, Austad SN,
1137 Chaudhuri AR. 2009. The long lifespan of two bat species is correlated with resistance to protein
1138 oxidation and enhanced protein homeostasis. *FASEB J* **23**: 2317-2326.
1139 Samaras N, Samaras D, Forster A, Frangos E, Philippe J. 2015. [Age related dehydroepiandrosterone
1140 decrease: clinical significance and therapeutic interest]. *Rev Med Suisse* **11**: 321-324.
1141 Satoh A, Brace CS, Rensing N, Cliften P, Wozniak DF, Herzog ED, Yamada KA, Imai S. 2013. Sirt1 extends
1142 life span and delays aging in mice through the regulation of Nk2 homeobox 1 in the DMH and
1143 LH. *Cell Metab* **18**: 416-430.
1144 Scharff A, Locker-Gruetjen O, Kawalika M, Burda H. 2001. Natural history of the Giant mole-rat,
1145 Cryptomys mechowi (Rodentia: Bathyergidae) from Zambia. *Journal of Mammalogy* **82**: 1002-
1146 1015.
1147 Schiaffino S, Mammucari C. 2011. Regulation of skeletal muscle growth by the IGF1-Akt/PKB pathway:
1148 insights from genetic models. *Skelet Muscle* **1**: 4.
1149 Schielke CKM, Burda H, Henning Y, Okrouhlik J, Begall S. 2017. Higher resting metabolic rate in long-lived
1150 breeding Ansell's mole-rats (Fukomys anselli). *Front Zool* **14**: 45.
1151 Schmidt CM, Blount JD, Bennett NC. 2014. Reproduction is associated with a tissue-dependent reduction
1152 of oxidative stress in eusocial female Damaraland mole-rats (Fukomys damarensis). *PLoS One* **9**:
1153 e103286.
1154 Seluanov A, Gladyshev VN, Vijg J, Gorbunova V. 2018. Mechanisms of cancer resistance in long-lived
1155 mammals. *Nat Rev Cancer* **18**: 433-441.
1156 Sherman PW, Jarvis JUM. 2002. Extraordinary life spans of naked mole-rats (Heterocephalus glaber).
1157 *Journal of Zoology* **258**: 307-311.
1158 Sichilima AM, Faulkes CG, Bennett NC. 2008. Field evidence for aseasonality of reproduction and colony
1159 size in the Afrotropical giant mole-rat Fukomys mechowii (Rodentia: Bathyergidae). *African*
1160 *Zoology* **43**: 144-149.
1161 Skliba J, Mazoch V, Patzenhauerova H, Hrouzková E, Lövy M, Kott O, Šumbera R. 2012. A maze-lover's
1162 dream: Burrow architecture, natural history and habitat characteristics of Ansell's mole-rat
1163 (Fukomys anselli). *MAMMALIAN BIOLOGY* **77**: 420-427.
1164 Starkov AA. 2008. The role of mitochondria in reactive oxygen species metabolism and signaling. *Ann N Y*
1165 *Acad Sci* **1147**: 37-52.
1166 Tacutu R, Craig T, Budovsky A, Wuttke D, Lehmann G, Taranukha D, Costa J, Fraifeld VE, de Magalhaes
1167 JP. 2013. Human Ageing Genomic Resources: integrated databases and tools for the biology and
1168 genetics of ageing. *Nucleic Acids Res* **41**: D1027-1033.
1169 Tatar M, Bartke A, Antebi A. 2003. The endocrine regulation of aging by insulin-like signals. *Science* **299**:
1170 1346-1351.
1171 Traish AM, Kang HP, Saad F, Guay AT. 2011. Dehydroepiandrosterone (DHEA)--a precursor steroid or an
1172 active hormone in human physiology. *J Sex Med* **8**: 2960-2982; quiz 2983.
1173 Valenzano DR, Terzibasi E, Genade T, Cattaneo A, Domenici L, Cellerino A. 2006. Resveratrol Prolongs
1174 Lifespan and Retards the Onset of Age-Related Markers in a Short-Lived Vertebrate. *Current*
1175 *Biology* **16**: 296-300.
1176 van Heemst D. 2010. Insulin, IGF-1 and longevity. *Aging Dis* **1**: 147-157.

1177 Väremo L, Nielsen J, Nookaew I. 2013. Enriching the gene set analysis of genome-wide data by
1178 incorporating directionality of gene expression and combining statistical hypotheses and
1179 methods. *Nucleic Acids Research* **41**: 4378-4391.
1180 Walker JJ, Spiga F, Gupta R, Zhao Z, Lightman SL, Terry JR. 2015. Rapid intra-adrenal feedback regulation
1181 of glucocorticoid synthesis. *J R Soc Interface* **12**: 20140875.
1182 Wang J, Mitsche MA, Lutjohann D, Cohen JC, Xie XS, Hobbs HH. 2015. Relative roles of ABCG5/ABCG8 in
1183 liver and intestine. *J Lipid Res* **56**: 319-330.
1184 Webb SJ, Geoghegan TE, Prough RA, Michael Miller KK. 2006. The biological actions of
1185 dehydroepiandrosterone involves multiple receptors. *Drug Metab Rev* **38**: 89-116.
1186 Zeugswetter F, Fenske M, Hassan J, Kunzel F. 2007. Cushing's syndrome in a guinea pig. *Vet Rec* **160**:
1187 878-880.

1188